The Lomagundi-Jatuli carbon isotopic event recorded in the marble of the Tandilia System basement, Río de la Plata Craton, Argentina

M.F. Lajoinie [a, b], M.E. Lanfranchini [a, c] *, C. Recio [d], A.N. Sial [e], C.A. Cingolani [b, f], C.A. Ballivián Juatiniano [a,b], R. O. Etcheverry [a, b]

[a] Instituto de Recursos Minerales, Facultad de Ciencias Naturales y Museo, Universidad Nacional de La Plata, INREMI-FCNyM-UNLP-CICBA, 64 N°3, (CP1900), Argentina. (*) lanfranchini@yahoo.com

[b] Consejo Nacional de Investigaciones Científicas y Técnicas, CONICET. Godoy Cruz, 2290, (C1425FQB) CABA, Argentina.

[c] Comisión de Investigaciones Científicas de la provincia de Buenos Aires, CICBA. 526 e/ 10 y 11 (CP 1900), La Plata, Argentina.

[d] Universidad de Salamanca. Patio de Escuelas 1, 37008, Salamanca, España.

[e] Department of Geology, Federal University of Pernambuco, NEG-LABISE, Recife, Brazil.

[f] Centro de Investigaciones Geológicas, CONICET-UNLP, Diagonal 113 N°275, La Plata, Argentina.

Abstract

The "Lomagundi-Jatuli event" corresponds to the most important $\delta^{13}C$ positive anomaly ($\geq 5‰$) globally reported in Palaeoproterozoic marine carbonates (between ~2.30 and 2.06 Ga). In the Tandilia System (Argentina), Río de la Plata Craton, this event was recorded in the basement marble of the San Miguel area. The calcite-diopside marble, hosted by biotite gneiss and intruded by 2.12 Ga garnet-leucogranite, was metamorphosed in amphibolite facies during the Transamazonian Cycle.

PAAS-normalised rare-earth elements (REE) and Y for the carbonate rocks are HREE-enriched and display positive Eu and Y anomalies, typical of primary precipitates from a mixed hydrothermal-marine environment carbonate. Additionally, a truly negative Ce anomaly for all the samples indicates that the depositional environment was oxidising.

Positive $\delta^{13}C$ values ranging from +5.90 to +4.30‰ (V-PDB), and $\delta^{18}O$ from +17.45 to +13.84‰ (V-SMOW) were determined in this marble, both gradually decreasing towards the contact with the leucogranites. These values indicate that devolatilization reactions took place during the crystallisation of a wollastonite-vesuvianite-grossular-diopside skarn generated by the leucogranite intrusions into the marble. $\delta^{18}O$ values obtained from diopside and calcite crystals, in the marble sectors furthest from the contacts with leucogranite, allowed a 663°C to 623°C formation temperature to be calculated, considering oxygen in a calcite-diopside geothermometric pair. These temperatures are consistent with the metamorphic degree (amphibolite facies) reached in this portion of the basement.

Although the San Miguel marble shows petrographic and mineralogical evidence of regional and contact metamorphism, important geochemical and isotopic characteristics,

together with its estimated Palaeoproterozoic age, indicate that the marble protolith was a marine carbonate deposited during the "Lomagundi-Jatuli event".

1. Introduction

The first stable isotope studies conducted on marine carbonates of the Lomagundi Group, Zimbabwe, which were deposited approximately in the 2.40-2.00 Ga interval, revealed an important positive anomaly in the $\delta^{13}C$ values (Schidlowski *et al.*, 1975, 1976). The anomaly was subsequently reported as much for well-preserved Palaeoproterozoic carbonates as others with superimposed metamorphism processes. This anomaly is of geological relevance, and was later named the "Lomagundi-Jatuli event" (LJE) by Melezhik *et al.* (2005).

Important advances in the knowledge of this event were accomplished in the Fennoscandian Shield (Fig. 1; Norway, Switzerland, and Finland) by Baker and Fallick (1989), Karhu (1993), and Melezhik and Fallick (1996); in Scotland by Baker and Fallick (1989); and in the North American Craton by Schidlowski *et al.* (1983), Mirota and Veizer (1994), Melezhik *et al.* (1997), and Bekker *et al.* (2003, 2006). Also, other outcrops from the South African cratons (Schidlowski *et al.*, 1976; Gauthier-Lafaye and Weber, 1989; Master *et al.*, 1990; Buick *et al.*, 1998, 2003; Bekker *et al.*, 2001; Schröder *et al.*, 2008; Master *et al.*, 2010; Martin *et al.*, 2013), the San Francisco Craton, Brazil (Bekker *et al.*, 2003; Maheshwari *et al.*, 2010), the Aravalli Craton, India (Maheshwari *et al.*, 1999, 2002, 2010), the north-eastern Sino-Korean Craton (Tang *et al.*, 2011), and from the Pilbara and Yilgarn Cratons, Australia (Lindsay and Brasier, 2002) have been studied (Fig. 1). Typically, these carbonates show $\delta^{13}C$ values between +5.00‰ and +16.00‰ or even higher (Lomagundi Group, Melezhik *et al.*, 2005). Although the beginning and duration of the "Lomagundi-Jatuli event" is still a matter of debate, records of stratigraphic and chemostratigraphic studies indicate that this event

4

started before 2.20 Ga, shortly after the Huronian glaciation ~2.45-2.22 Ga (Young *et al.*, 2001) and the Great Oxidation Event 2.45-2.32 Ga (Holland, 2002; Bekker *et al.*, 2003), and finished around 2.11-2.06 Ga (Bekker *et al.*, 2008), extending for more than 300 Ma (Karhu and Holland, 1996; Melezhik *et al.*, 2005, 2007). During this period, an increase in the organic C production consequently released to the oceans and atmosphere, accompanied by an increase in the O levels, produced C oxidation, generating important modifications both in the environment and in biological processes (Karhu and Holland, 1996). Thus, the characterisation of the space and time distribution of "Lomagundi-Jatuli event" carbonates is still an essential tool for the correlation and understanding of the processes that generated one of the most important modifications to the C cycle worldwide during the Palaeoproterozoic period.

This anomaly was also recognized by Maheshwari *et al.* (2010) in the Piedra Alta terrane, Uruguay, Río de la Plata Craton (Fig. 1; RPC). The carbonate is predominantly dolomitic, and lays in the San José Belt (Bossi *et al.*, 1993, 1998; Bossi and Cingolani, 2009), constituting a sedimentary succession that corresponds to the Paso Severino Formation. The unit has a depositional SHRIMP U-Pb age of 2.14 ± 0.21 Ga (obtained from meta-rhyolites from the top of this formation; Hartmann *et al.*, 2000a). Also, a minimum SHRIMP U-Pb age of 2.07 ± 0.06 Ga has been obtained from the Isla Mala granodiorite (Hartmann *et al.*, 2000a). The carbonate has a wide range of $\delta^{13}C$ values varying from -5.00 to +11.60‰. Although the positive $\delta^{13}C$ values are typical of the Palaeoproterozoic carbonates, the negative ones would be associated with remineralisation of the organic matter in early diagenetic environments (Maheshwari *et al.*, 2010).

5

In this work, we report $\delta^{13}C$ and $\delta^{18}O$ data, together with rare earth elements and Y analyses of basement marble of the San Miguel area, Tandilia System (Argentina), in order to stablish the marble origin and its relationship with the Lomagundi-Jatuli isotopic event.

2. Geological setting

2.1 Río de la Plata Craton

The Río de la Plata Craton (RPC; Almeida *et al.*, 1973; Rapela *et al.*, 2007; Cingolani, 2010) is located in South America, and it is mainly exposed in Uruguay, Paraguay, south-eastern Brazil, and to some extent in Argentina (Fig. 2a). The Craton is composed of dominated Palaeoproterozoic (Rhyacian) igneous-metamorphic units (Cordani *et al.*, 2000; Rapela *et al.*, 2007), possible Archaean nuclei (Hartmann *et al.*, 2000b; Cingolani, 2010), and Mesoproterozoic belts and rocks (Oyhantçabal *et al.*, 2005; Gaucher *et al.*, 2011) mostly covered by Neoproterozoic to Lower Paleozoic sedimentary rocks, Cretaceous basalts from the Paraná basin, and by modern sediments restricted to some sectors.

The RPC was affected by two major cycles that correspond to the Transamazonian (or Transplatense, Santos *et al.*, 2017), 2.20-1.70 Ga, and the Brazilian, 0.80-0.50 Ga (Brito Neves *et al.*, 2014; Dalla Salda *et al.*, 1988; Pimentel and Fuck, 1992; Bossi *et al.*, 1993; Hartmann *et al.*, 2002a).

The westernmost edge of the RPC is in contact with the Pampia terrane in Argentina (Rapela *et al.*, 2007; Favetto *et al.*, 2015; Fig. 2a) and in Paraguay (Caapuçú or Tebycuary High; Fulfaro, 1996; Fig. 2a), while the eastern limit crops out in southern

6

Brazil, Encantadas-Tacuarembó domains (Hartmann *et al.*, 2007; Santos *et al.*, 2017), Curitiba and Luís Alves microcratons (Siga Júnior *et al.*, 2007), and in Uruguay in the Piedra Alta terrane (Santos *et al.*, 2003; Chernicoff *et al.*, 2014), Nico Pérez terrane (Gaucher *et al.*, 2009; Bossi and Cingolani, 2009; Santos *et al.*, 2017) and Rivera block (the last one is considered part of the Tacuarembó domain, Santos *et al.*, 2017) (Fig. 2b). The southernmost outcrops of the RPC are exposed in Argentina, at Martín García Island (Fig. 2a) and in the Tandilia region, (Fig. 2c; Dalla Salda *et al.*, 2005; Pankhurst *et al.*, 2003; Rapela *et al.*, 2007). However, some authors suggest, based on geochronological data, that the boundary of the RPC could be extended further south (to the limit with the Patagonia terrane; Ramos, 1988; Tohver *et al.*, 2012) and further north (Paranapanema domain, Santos *et al.*, 2017).

2.2 Tandilia System

The Tandilia System comprises a group of hills that reach 500 m above sea level, and are distributed along 350 km in a northwest-southeast direction. The set of rocks exposed in these hills corresponds predominantly to a Palaeoproterozoic basement covered by a sedimentary sequence of Lower Neoproterozoic to Silurian age (Fig. 2c).

The basement, named the Buenos Aires Complex (Marchese and Di Paola, 1975), consists mainly of igneous and metamorphic rocks. The igneous rocks are acidic to intermediate granitoids with a great variability in their mineralogy and texture. They have a SHRIMP U-Pb age of 2.10-2.18 Ga (Chernicoff *et al.*, 2015; Cingolani *et al.*, 2002; Hartmann *et al.*, 2002a and b) and an Rb-Sr age between 2.15 and 1.77 Ga (Hart *et al.*, 1965; Halpern *et al.*, 1970; Linares and González, 1990; Pankhurst *et al.*, 2003). The metamorphic rocks correspond to granitic and tonalitic gneisses (with varied

7

characteristics), migmatites, amphibolites and scarce schists, marbles, and skarns. Mylonitic zones have also been described (Villar Fabre, 1954; Teruggi and Kilmurray, 1975; Cingolani and Dalla Salda, 2000) concentrated in two E-W trending belts: the Azul Megashear Zone that crops out along a 40 km stretch south of Azul city (Frisicale *et al.*, 1999), and a 25-km-long belt located south of Tandil city (Dalla Salda, 1981).

The most extensive outcropping metamorphic rocks of the region are located in the Balcarce area (Fig. 2c) and correspond to garnet gneisses, which have a SHRIMP U-Pb age of 2.17-2.07 Ga (Cingolani *et al.*, 2002; Hartmann *et al.*, 2002a). These rocks have variable fabrics that ranges from strongly foliated to massive or isotropic (Dalla Salda *et al.*, 2005). The mineralogy includes plagioclase, potassium feldspar, quartz, garnets and/or biotite, and eventually pyroxene; also, some varieties of these gneisses comprise muscovite and sillimanite (Dalla Salda *et al.*, 2005). These rocks exhibit evidence of partial melting, such as quartz-feldspathic concordant and discordant small bodies, and/or sectors enriched with mafites, garnet, and epidote (Dalla Salda *et al.*, 2005).

Migmatites are frequently found, however, they are difficult to identify since they are closely related to with gneisses and granitic rocks. They are made up of quartz-feldspar leucosomes, sometimes with neoformed garnets, and have Sm-Nd ages of 2.14 ± 0.88 Ga (Pankhurst *et al.*, 2003). Structures are diverse and vary from stromatic to nebulitic (Dalla Salda *et al.*, 2005). Amphibolites occur as isolated bodies or xenoliths, included within the gneisses or the granitic plutons, in the central portion of the Tandilia System. They are composed of plagioclases, quartz, amphibole, epidote, and biotite (Quartino and Villar Fabre, 1967; Delpino, 2000; Dalla Salda *et al.*, 2005). Schists are scarce, mainly micaceous, and they are found in the Balcarce and Azul city areas (Teruggi and Kilmurray, 1980).

8

Two types of marbles have been identified: dolomite marble at Punta Tota, Balcarce city (Delpino and Dristas, 2008), and calcite marble at San Miguel, near Tandil city (Quartino and Villar Fabre, 1967; Lajoinie *et al.*, 2013, 2014b; Lajoinie, 2015) (Fig. 2c). Both marbles show evidence of metasomatism, with further formation of skarns. Geothermobarometric data, obtained by Delpino and Dristas (2008) from dolomites and associated calc-silicate rocks of Punta Tota area, indicate metamorphic conditions of 750-800°C and 5-6kbar, followed by an isobaric cooling to 450-500°C.

A set of low-grade metamorphic rocks (low greenschist facies) which consists of metacherts, metagreywackes, and metabasalts (El Cortijo Formation, Teruggi *et al.*, 1988; Lajoinie *et al.*, 2017) crops out in the SW area of Tandil city (Fig. 2c). These rocks have been interpreted as the remaining portion of the oceanic crust linked to an island arc accreted to the Tandilia terrane during the Transamazonian Cycle (Teruggi *et al.*, 1988).

A Neoproterozoic sedimentary cover, composed of a calcareous-siliciclastic succession, overlays this basement (Fig. 2c). It comprises the Sierras Bayas Group (Dalla Salda and Iñiguez, 1979; Poiré *et al.*, 1984; Poiré, 1993) and the La Providencia Group, with ages of ~0.90-0.80 Ga to 0.58 Ga (Poiré, 1987; Gómez Peral *et al.*, 2007; Gómez Peral, 2008), and ~0.56-0.41 Ga (Iñiguez and Zalba, 1974; Gómez Peral *et al.*, 2005; Arrouy *et al.*, 2016a and b), respectively. On the top of the above-mentioned succession, the Balcarce Formation occurs. It consists of a siliciclastic sequence of Lower Cambrian to Silurian age (Teruggi *et al.*, 1958; Poiré *et al.*, 2003; Seilacher *et al.*, 2002; Zimmermann and Spalletti, 2009; Cingolani, 2010). Both successions (calcareous-siliciclastic and siliciclastic) correspond to a marine platform environment (Poiré, 1987; Poiré *et al.*, 2003).

9

2.3 Metamorphic and tectonic settings

The tectono-magmatic evolution of the basement occurred during the Transamazonian Cycle or its equivalent in Argentina, the Tandileano Cycle (Teruggi and Kimurray, 1975; Dalla Salda *et al.*, 1988; Ramos, 1999). It is linked to the accretion of the Tandilia terrane, on the southern margin of the BA-PA terrane (Teruggi *et al.*, 1988; Dalla Salda *et al.*, 1988), that generated deformation, metamorphism (amphibolite to granulite facies), and anatexis of cortical rocks (Dalla Salda and Franzese, 1989; Cingolani and Dalla Salda, 2000; Cingolani, 2010). Recently, Chernicoff *et al.* (2014) interpreted the evolution history previous to the 2.00 Ga collision through geophysical studies. These authors point out that a rift system initiated in the Neoarchaean-Siderian would have separated the Tandillia terrane of the RPC, generating an ocean basin (Fig. 3a). Afterwards, between 2.37 and 2.17 Ga (early Rhyasian), the beginning of a subduction towards the north of Tandilia, and another intraoceanic subduction, determined the formation of a continental magmatic arc and an island arc (El Cortijo, Teruggi *et al.*, 1988; Cingolani, 2010), respectively (Fig. 3b). This episode ended at 2.0 Ga (late Rhyasian), with the collision of the Tandilia terrane with the southern margin of the BA-PA terrane (Fig. 3c) (Cingolani, 2010; Chernicoff *et al.*, 2014). Then, a tensional stage occurred during the Neoproterozoic to Lower Cambrian period when an important faulting affected the Palaeoproterozoic basement and, partly, the sedimentary cover (Cingolani, 2010).

2.4 San Miguel area

The San Miguel (SM) area is located 60 km southwest of Tandil city (Fig. 2c). It comprises basement outcrops, surrounded by an extended modern sedimentary cover (Fig. 4). The most widespread rocks are biotite gneiss, migmatites (Rb-Sr age of 2.12 ± 0.01 Ga; Halpern *et al.*, 1970), calcitic marble, and a wollastonite-vesuvianite-grossular-diopside skarn (Lajoinie, 2015) (Fig. 4). Also, igneous rocks crop out in the area as tonalite and granite bodies, and an andesite-basaltic dike (Lajoinie *et al.*, 2014a).

The biotite gneiss displays a heterogeneous colouration with pale and dark tonalities of grey, medium-coarse grain size and equigranular texture. It shows a planar anisotropic fabric of compositional banding type (S_1), given by the alternation of pale and dark bands orientated in a N35°E direction and 60°SW inclination (Fig. 5a). The pale bands are whitish, approximately 2-3 cm wide and are composed of quartz, K-feldspar, and plagioclase, while the dark ones are black or grey, approximately 4 cm wide, and contain abundant biotite besides the above-mentioned minerals (Fig. 5b).

The migmatites generally exhibit stromatic structures produced by the alternation of leucosome bands (parallel to S_1 foliation) with mesosomes that corresponds to the biotite gneiss (Fig. 5c). The leucosomes are composed of quartz, K-feldspar, and plagioclase crystals of coarse grain size; also, garnets are observed in some of the more voluminous leucosomes (Fig. 5d). Commonly, these bodies exhibit a whitish to greyish colouration, with medium to coarse grain size and porphyroblastic texture in response to the presence of reddish-brownish garnet porphyroblasts up to 1 cm in diameter (Fig. 5d).

The marble (Fig. 6a) has whitish to grey colouration and is mostly composed of calcite, and a lesser extent by a green-coloured clinopyroxene. It is in contact with the gneiss and is intruded by migmatite leucosomes or leucogranites (Fig. 6a and b). Leucogranites

11

have a "sill" morphology that repeatedly cuts the marble, developing numerous marble-layered bodies of 1- to 2-m-wide (Fig. 6b and c). A calc-silicate paragenesis, consisting of wollastonite+vesuvianite+grossular+diopside, developed in each contact marble-leucogranite, forming the San Miguel skarn (Fig. 6d; Lajoinie *et al.*, 2013).

3. Analytical methods and sample locations

A total of 12 representative samples of the SM marble were selected for petrographic studies and eight for geochemical characterisation. The sampling pattern followed a cross-section in the marble that went from the furthest to the nearest sectors, to the contact with leucogranite bodies (Fig. 7a and b). The composition of the clinopyroxene crystals was determined using an electron microprobe Cameca, Camebax SX 100 model, in the microanalysis laboratory of the Servicio de Ciencia y Técnica de la Universidad de Oviedo, Spain. Operating conditions were 20 kv accelerating voltage, beam current of 20 nA, and beam size of 1 to 2 μm. Natural standards certificated by MAC (Micro Analysis Consultants Ltd. United Kingdom) were used for calculating element concentrations: albite for Na and Si, Al_2O_3 for Al, MgO for Mg, andradite for Ca, orthoclase for K, synthetic Mn and Ti oxides for Mn and Ti, magnetite for Fe, NiO for Ni and chromite for Cr.

Geochemical analyses of the samples, previously crushed and pulverised to 200 mesh in a ring mill, were carried out at the Laboratorio ALS Patagonia S.A. (Argentina). Major elements (SiO_2, TiO_2, Al_2O_3, Fe_2O_3, MnO, MgO, CaO, Na_2O, K_2O, and P_2O_5) were determined by X-ray fluorescence spectrometry following the ME-XRF12 routine, where the samples were calcined and dissolved with 50% $Li_2B_4O_7$-50% $LiBO_2$, and

12

finally melted at 1050-1100ºC until forming a pearl. The standards used were SARM-39 and SARM-45. Elements such as Ba, Cr, Rb, Cs, Ga, Hf, Nb, Y, Sr, Sn, Ta, Th, U, V, W, Zr, and REE were determined following the ME-MS81 routine, which consists of mixing 0.20 g of the sample with 0.90 g of $LiBO_2$ and melting them at 1000ºC. The solution obtained was cooled and dissolved in 100 ml of 4% HNO_3-2% HCl and then analysed using inductively-coupled plasma mass spectrometry (ICP-MS).

Isotopic determinations of $\delta^{13}C$ and $\delta^{18}O$ were conducted at the Servicio de Isótopos Estables de la Universidad de Salamanca (Spain) using a SIRA-II gas source mass spectrometer, manufactured by VG-Isotech and equipped with *cold finger* to analyse small samples and a multiple system of sample admission. The mineral samples (calcite and diopside) were separated and concentrated by hand-picking under a binocular microscope from other fractions of the same samples used for chemical analyses. For the gas extraction (CO_2) a reaction with 103% H_3PO_4 at 25°C for 12 hours was used. Conventional methodologies according to Clayton and Mayeda (1963) were used for the treatment of the diopside crystals. The isotopic relationships are reported in delta notation (δ ‰) relative to the V-PDB (*Pee Dee Belemnite*) standard for the $\delta^{13}C$, and to the V-SMOW (*Standard Mean Ocean Water*) for the $\delta^{18}O$, with an analytical error of ± 0.2‰.

Sm-Nd isotopic dating on garnet-whole rock pairs of two skarn samples was performed at the Laboratório de Geocronologia, Universidade de Brasília (Brazil), according to the methodology proposed by Gioia and Pimentel (2000).

The samples were pulverised and their Sm and Nd contents were first determined using X-ray fluorescence. The extraction of the elements (Sm and Nd) was done using conventional cation exchange techniques, and then loaded onto Re evaporation

13

filaments of double filament assemblies. The isotopic measurements were performed on a multicollector Finnigan MAT 262 mass spectrometer in static mode. The uncertainties for the $^{147}Sm/^{144}Nd$ and $^{143}Nd/^{144}Nd$ ratios are better than $\pm$ 0.2% (2σ) and $\pm$ 0.005% (2σ), respectively. $^{143}Nd/^{144}Nd$ ratios were normalised to an $^{146}Nd/^{144}Nd$ ratio of 0.7219 and the decay constant used was $\lambda^{147}Sm = 6.54 \times 10^{-12}$ a^{-1}.

4. Petrography of marble

The marble has an inequigranular coarse-grained texture ranging from 2 mm to ~30 mm grain size. Its mineralogy is mostly composed of calcite, with small amounts of clinopyroxene of a diopside type ($di_{62.32-79.60}$ $hd_{20.23-37.43}$ $jo_{<0.25}$; Table 1) and scarce quartz (Fig. 8a).

The calcite crystals are well developed; they have intracrystalline deformation as evidence of undulose extinction, and tapered and deformed lamellae twins (Fig. 8b). Also, some calcite crystals show mechanical twinning of crossing and stopping types (Chen *et al.*, 2011; Fig. 8c). Diopside is dark green, with a medium crystal length of 3-4 mm and has a slightly variable abundance between 10 and 15%. Some crystals are replaced by chlorite and amphibole, of tremolite type (Fig. 8d). Scarce and isolated quartz crystals of 0.5 mm average size are present, showing undulose extinction (intracrystalline deformation) and subgrain presence (recovery) (Fig. 8b). Apatite occurs as accessory minerals.

5. Geochemical characterisation of marble

5.1 Major and trace elements

Bulk rock chemical analyses for all samples are presented in Table 2. The studied marble exhibits high contents of CaO (51.60 to 54.80 wt.%), in agreement with the great amount of calcite identified. Low SiO_2 (1.62 to 8.65 wt.%), MgO (0.53 to 1.13 wt.%), and Fe_2O_3 (0.13 to 1.63wt.%) contents are attributed to the presence of diopside and quartz crystals. In addition, low Al_2O_3 (< 1.22 wt.%), Ti_2O (<0.04 wt.%), Hf (< 0.30 ppm), Th (< 0.59 ppm), and Zr (< 14 ppm) contents residing in the terrigenous silicate fraction were found. Samples are also depleted in trace elements, except for Ba and Sr, which show a wide variation between 10.4 and 1080.0 ppm, and 115.0 and 303.0 ppm, respectively. Finally, a slightly negative correlation exists for CaO vs. Sr (Fig. 9a) and positive for ∑REE vs. Al_2O_3 (Fig. 9b) and Ti_2O vs. Zr (Fig. 9c).

5.2 REE and Y

Rare earth elements and Y data are shown in Table 3. These contents were normalised to Post-Archaean Average Australian Shale (PAAS; Taylor and MacLennan, 1985) and plotted in Fig. 10. These samples have very low ∑REE contents (7.43-53.34 ppm), slight enrichment of HREE (Pr/Yb_{PAAS} 0.55-1.00), and MREE (Sm/Yb_{PAAS}) contents of 0.67 to 1.64. Only a-SMC and SMC-1 samples show HREE contents of 1.94 and 1.05 ppm. The studied samples also have positive Eu/Eu* anomalies between 1.53 and 2.97 (Eu/Eu* according to Bau and Dulski, 1996) and truly negative Ce anomalies on the basis of Ce/Ce* <1 and Pr/Pr* >1 in all cases (following Bau and Dulski's, 1996 method). Finally, the La/La* (1.27-2.00, after Bolhar *et al*., 2004) and Y (Y/Ho 47.06-70.84) anomalies are positive.

15

5.3 $\delta^{13}C$ and $\delta^{18}O$ isotopes

All $\delta^{18}O$ values obtained from marble calcite crystals are positive and range between +17.45 and +13.84‰ (V-SMOW), whereas the $\delta^{13}C$ contents are also remarkably positive and vary between +5.89 and +4.26‰ (V-PDB), as indicated in Table 4. This table also includes data obtained from Lajoinie *et al.* (2014b). The values plotted in a $\delta^{13}C$ vs. $\delta^{18}O$ diagram (Fig. 11) show the fluid evolution in isotopic equilibrium with calcite. A correlation between isotopic values and its position with respect to the marble-leucogranite contact is highlighted in the diagram. The correlation shows that the most positive values of $\delta^{13}C$ and $\delta^{18}O$ correspond to the samples located furthest from the above-mentioned contact.

$\delta^{18}O$ (V-SMOW) data from marble diopside is shown in Table 4. The diopside $\delta^{18}O$ values (+14.90, +14.70, and +14.50‰) together with those obtained for calcite from the same samples (+17.45, +17.12, and +16.80‰ V-SMOW) allowed the isotopic equilibrium temperature to be determined using the calcite-diopside geothermometer proposed by Zheng (1993). These results indicate temperatures of 623°C to 663°C (Table 4).

5.4 Sm-Nd

Two garnet-whole rock pairs of skarn samples were analysed using the Sm-Nd method (Table 5); however, reliable ages could not be obtained. The Nd model ages related to the depleted mantle (T_{DM}) of the studied skarn are 2.47 Ga and 3.05 Ga. The model ages of sedimentary rocks reflect average crustal residence ages of their source region (Goldstein *et al*., 1997). In this sense, the Nd model ages of skarn samples from the San Miguel area are similar to those obtained by Pankhurst *et al*. (2003) for other basement

units of the Tandilia System in the Olavarría area (T_{DM} = 2.46-2.52 Ga). Our results

provide reliable evidence of participation of a Siderian or older basement in the

formation of the studied rocks, since the real value characterising the moment of

separation of material from the evolutionary line of the depleted mantle could be older

(*e.g.* Arndt and Goldstein, 1987).

6. Discussion

Palaeoproterozoic carbonates deposited during the "Lomagundi-Jatuli event" (2.22 to

2.06 Ga; Karhu and Holland, 1996) have been recognized in several formations

belonging to different cratonic units around the world, due to the presence of an

important positive anomaly in the $\delta^{13}C$ ($\geq$+5‰) values.

In the San Miguel area, one of the two unique carbonate rocks which form part of the

Palaeoproterozoic crystalline basement of the Tandilia System, Río de la Plata Craton,

crops out. The marble has a calcite+diopside+quartz± apatite mineral association and is

in contact with the biotite gneiss and intruded by leucogranites (2.12 ± 0.01 Ga Rb-Sr

age; Halpern *et al.*, 1970). Considering the presence of a high-grade metamorphic rock

assemblages and the diopside isograde temperature obtained (~650°C, for 8 Kbars P,

Bucher and Frey, 2002), the regional metamorphic processes must have reached an

amphibolite facies grade. These metamorphic processes also generated calcite crystal

deformations and compositional banding (S_1) formation in the gneiss. According to the

regional tectonic context of the Tandilia System, this episode corresponds to the

Transamazonian Orogeny (2.20-1.80 Ga; Dalla Salda *et al.*, 2005). This assertion is

supported by the Rb-Sr age of the leucogranites (consistent with the ages obtained for

other basement gneisses and migmatites), which could be considered the mínimum depositional age for the marble. Furthermore, the provenance of the marble may have a 2.47 to 3.05 Ga component or source according to the Nd model ages. In addition, Rapela *et al.* (2007), Gaucher *et al.* (2008), and Cingolani (2010) performed U-Pb ages obtained from detrital zircons near the study area. Detrital zircons were sampled from the base of the Sierras Bayas Group, more precisely from the "Lower quartzites" of the Villa Mónica Formation, which overlays the metamorphic basement rocks (Poiré, 1993). These determinations show a unimodal Palaeoproterozoic age indicating that this formation was mostly derived from the underlying basement, which has a restricted age range (Cingolani, 2010).

Although the metamorphism has generated some modifications in the chemical patterns of the studied marble, the chemical analyses show some particularities that correspond to the primitive characteristics of the marble protolith. The abundance of CaO and the low contents of the other majority oxides indicate that the marble is almost calcitic. Also, low contents of terrigenous silicate fraction elements (Al_2O_3, Ti_2O, Hf, Th, and Zr) indicate that the REE +Y values in the marble reflect marine conditions (Alexander *et al.*, 2008; Bolhar *et al.*, 2004; Bau and Dulski, 1996). Positive Eu anomalies are typical in Archaean-Palaeoproterozoic precipitates, and manifest the high hydrothermal fluid activity in the oceans for that period (Alexander *et al.*, 2008). Moreover, the presence of positive Y anomalies is also characteristic of seawater precipitates (Nosaki *et al.*, 1997), while negative Ce anomalies indicate an oxidative precipitation environment for the carbonate protolith. In these conditions, Ce^{+3} is oxidised to Ce^{+4} (less soluble), and is consequently removed from the solution by suspended particles (Bolhar *et al.*, 2004). In this sense, the Archaean-Palaeoproterozoic transition was

18

indicated as a period when free atmospheric di-oxygen became relatively abundant (Fig. 12a; Cloud, 1968; Martin *et al.*, 2013) based on the appearance of oxidised "red" beds in sedimentary successions, and the disappearance of detrital uraninite, siderite, and pyrite (Fig. 12b; Cloud, 1972; Martin *et al.*, 2013). This event, called the Great Oxidation (Holland, 2002), occurred between 2.50 and 2.32 Ga and was followed by the Lomagundi-Jatuli event (2.20-2.06 Ga) (Fig. 12).

$\delta^{13}C$ stable isotope data obtained from calcite crystals revealed an important positive anomaly (Fig. 12c), confirming the marine origin of the marble suggested by Lajoinie *et al.* (2013, 2014b). According to these results, a decrease in the $\delta^{13}C$ (from +5.89 to +4.26‰) and in the $\delta^{18}O$ values (from +17.85 to +13.84‰) is observed towards the contact between the marble and leucogranite intrusions. Although many of the LJE carbonates remain unaltered, others show evidence of diagenetic and even metamorphic processes. According to several studies (Baker and Fallick, 1989; Melezhik *et al.*, 2001; Melezhik and Fallick, 2010), the original $\delta^{13}C$ and $\delta^{18}O$ values can be modified or remain almost unaltered even under amphibolite facies conditions, depending on metamorphic conditions and on the carbonate rock compositions. In the study area, the presence of a wollastonite-vesuvianite-grossular-diopside skarn (Lajoinie *et al.*, 2013) suggests that the calc-silicate mineral formation, produced by devolatilization reactions (Valley, 1986), may be the cause of the decreasing patterns registered in the $\delta^{13}C$ and $\delta^{18}O$ values. Normally, when calc-silicates form, CO_2 released from the carbonate is enriched in ^{13}C and ^{18}O (Shieh and Taylor, 1969). However, the $\delta^{13}C$ contents are not significantly modified given that it is more strongly influenced by carbonate rocks than by CO_2 content in leucogranite-derived fluids. In metasomatic processes, the oxygen isotope values are the most sensitive to modification, but there is up to 2 to 4‰

19

permissible $\delta\ ^{18}O$ depletion, called the "calc-silicate limit" (Valley, 1986). Thus the ~ +18‰ $\delta^{18}O$ values originally registered could have been around 20-22‰.

$\delta^{18}O$ values obtained from marble diopside crystals allowed a temperature range of 663°C-623°C to be determined, using the geothermometric calcite-diopside pair, which is in accordance with the 716ºC temperature obtained by Lajoinie *et al.* (2014a), and with the above-mentioned high degree of amphibolite facies, estimated for the SM outcropping rocks.

7. Conclusions

1. Positive Eu and Y anomalies, together with a slight enrichment of MREE and HREE (with respect to LREE), indicate that the SM marble protolith would have been formed by chemical precipitation from mixed hydrothermal and marine fluids during the Palaeoproterozoic era.

2. The Ce negative anomaly indicates oxidising conditions for precipitation environments, which is consistent with the relatively more-abundant free atmospheric oxygen for the period.

3. $\delta^{13}C$ and $\delta^{18}O$ values show decreasing patterns provoked by metamorphic and metasomatic processes. However, $\geq+5$‰ $\delta^{13}C$ values and closer to 18‰ $\delta^{18}O$ values together with the Palaeoproterozoic estimated age indicate that the SM marble was derived from a marine carbonate deposited during the "Lomagundi-Jatuli event".

4. The presence of Lomagundi-Jatuli marble in the Tandilia System basement constitutes a new correlation element between the Rio de la Plata Craton and other

20

Archaean-Palaeoproterozoic Cratons, and even among other carbonate rocks in the same Craton.

References

Arndt, N.T., Goldstein, S.T., 1987. Use and abuse of crust-formation ages. Geology 15, 893-895.

Alexander, B.W., Bau, M., Andersson, P., Dulski, P., 2008. Continentally-derived solutes in shallow Archean seawater: rare earth element and Nd isotope evidence in iron formation from the 2.9 Ga Pongola Supergroup, South Africa. Geochemica et Cosmochemica Acta 72, 378-394.

Almeida, F.F.M., Amaral, G., Cordani, U.G., Kawashita, K., 1973. The Precambrian evolution of the South American cratonic margin, south of the Amazon River, in: Nairn AE, Stehli FG (Eds.), The ocean basins and margins, vol 1. Plenum Publishing, New York, 411-446.

Arrouy, M.J., Poiré, D.G., Gómez Peral, L.E., Canalicchio, J.M., 2016a. Sedimentología y estratigrafía del grupo La Providencia (nom. nov.): cubierta superior neoproterozoica, sistema de Tandilia, Argentina. Latin American Journal of Sedimentology and Basin Analysis 22, 171-189.

Arrouy, M.J., Warren, L. V., Quaglio, F., Poiré, D.G., Simões, M.G., Rosa, M.B., Gómez Peral, L.E., 2016b. Ediacaran discs from South America: probable soft-bodied macrofossils unlock the paleogeography of the Clymene Ocean. Scientific Reports, v. 6, p. 30590, doi: 10.1038/srep30590. http://www.nature.com/articles/srep30590.

Baker, A.J., Fallick, A.E., 1989. Heavy Carbon in 2-Billion-Year-Old Marbles from Lofoten-Vesteralen, Norway. Implications for the Precambrian Carbon-Cycle. Geochimica et Cosmochimica Acta 53, 1111-1115.

Bau, M., Dulski, P., 1996. Distribution of yttrium and rare earth elements in the Penge and Kuruman iron-formations, Transvaal Supergroup, South African Earth. Precambrian Research 72, 235-245.

Bekker, A., Kaufman, A.J., Karhu, J.A., Beukes, N.J., Swart, Q.D., Coetzee, L.L., Eriksson, K.A., 2001. Chemostratigraphy of the Paleoproterozoic Duitschland Formation. South Africa: implications for coupled climate change and carbon cycling. American Journal of Science 301, 261-285.

Bekker, A., Sial, A.N., Karhu, J.A., Ferreira, V.P., Noce, C.M., Kaufman, A.J., Romano A.W., Pimentel, M.M., 2003. Chemostratigraphy of carbonates from the Minas Supergroup, Quadrilatero Ferrifero (Iron Quadrangle), Brazil: a stratigraphic record of early Proterozoic atmospheric, biogeochemical and climatic change. American Journal of Science 303, 865-904.

Bekker, A., Karhu, J.A., Kaufman, A.J., 2006. Carbon isotope record for the onset of the Lomagundi carbon isotope excursion in the Great Lakes area, North America. Precambrian Research 148, 145-180.

Bekker, A., Holmden, C., Beukes, N.J., Kenig, F., Eglington, B., Patterson, W.P., 2008. Fractionation between inorganic and organic carbon during the Lomagundi (2.22-2.1Ga) carbon isotope excursion. Earth and Planetary Science Letters 271, 278-291.

Bekker, A., Holland, H.D., 2012. Oxygen overshoot and recovery during the early Palaeoproterozoic. Earth Planet Science Letters 317, 295-304.

Bolhar, R., Kamber, B.S., Moorbath, S., Fedo, C.M., Whitehouse, M.J., 2004. Characterization of early Archaean chemical sediments by trace elements signatures. Earth and Planetary Science Letters 222, 43-60.

Bossi, J., Preciozzi, F., Campal, N., 1993. Predevoniano del Uruguay Parte 1: Terreno Piedra Alta. Dinamige, 50 p., Montevideo.

Bossi, J., Ferrando, L., Montaña, J., Campal, N., Morales, H., Gancio, F., Schipilov, A., Piñeyro, D., Sprechmann, P., 1998. Carta geológica del Uruguay, Escala 1:500.000 Geoeditores, Montevideo.

23

Bossi, J., Cingolani, C., 2009. Extension and general evolution of the Río de la Plata Craton, in: Gaucher, C., Sial, A.N., Halverson, G.P., Frimmel, H.E. (Eds.), Neoproterozoic-Cambrian tectonics, global change and evolution: a focus on southwestern Gondwana. Developments in Precambrian Geology, Elsevier 16, 73-85, Amsterdam.

Bowman, J.R., 1998. Stable-Isotope systematics of skarns, in: Lentz, D.R. (Ed.), Mineralized Intrusion Related Skarn Systems, Mineralogical Association of Canada. Short Course 26, 99-145, Québec.

Brito Neves, B.B., Fuck, R.A., Pimentel, M.M., 2014. The Brasiliano collage in South America: a review. Brazilian Journal of Geology, 44, 493-518.

Bucher, K., Frey, M., 2002. Petrogénesis of Metamorphic Rocks. Springer-Verlag Berlin Heidelberg, 341 p., Nueva York.

Buick, I.S., Uken, R., Gibson, R.L. and Wallmach, T., 1998. High δ^{13}C Paleoproterozoic carbonates from the Transvaal Supergroup, South Africa. Geology 26, 875-878.

Buick, I.S., Williams, I.S., Gibson, R.L., Cartwright, I., Miller, J.A., 2003. Carbon and U-Pb evidence for a Palaeoproterozoic crustal component in the Central Zone of the Limpopo Belt, South Africa. Journal of Geological Society of London 160, 601-612.

Chen, K., Kunz, M., Tamura, N., Wenk, H., 2011. Deformation twinning and residual stress in calcite studied with synchrotron polychromatic X-ray microdiffraction. Physics and Chemistry of Minerals 38, 491-500.

Chernicoff, C.J., Zappettini, E.O., Peroni, J., 2014. The Rhyacian El Cortijo suture zone: aeromagnetic signature and insights for the geodynamic evolution of the southwestern Río de la Plata craton, Argentina. Geoscience Frontiers 5, 43-52.

Chernicoff, C.J., Pereyra, F., Santos, J:O:S., Zappettini, E.O., 2015. Primeras edades U-Pb SHRIMP del Cratón del Río de la Plata en el subsuelo del area metrolpolitana de Buenos Aires. Revista de la Asociación Geológica Argentina, Nota Breve, 72, 575-577.

Cingolani, C.A., 2010. The Tandilia System of Argentina as a southern extension of the Río de La Plata Craton: An overview. International Journal of Earth Sciences 100, 221-242.

Cingolani, C.A., Dalla Salda, L.H., 2000. Buenos Aires cratonic region, in: Cordani, U., Milani, E., Thomaz Filho, A., Campos, D. (Eds.), Tectonic evolution of South America. 31st International Geological Congress, 139-146, Río de Janeiro.

Cingolani, C.A., Hartmann, L.A., Santos, J.O.S., McNaughton, N.J., 2002. U-Pb SHRIMP dating of zircons from the Buenos Aires complex of the Tandilia belt, Río de la Plata Craton, Argentina. 15° Congreso Geológico Argentino, Actas, 149-154, El Calafate.

Clayton, R.N., Mayeda, T.K., 1963. The use of bromine pentafluoride in the extraction of oxygen from oxides and silicates for isotopic analysis. Geochemica et Cosmochemica Acta 27, 43-52.

Cloud, P.E., 1968. Atmospheric and hydrospheric evolution on the primitive Earth. Science 160, 729-736.

Cloud, P.E., 1972. A working model of the primitive Earth. American Journal of Science 272, 537-548.

Cordani, U.G., Sato, K., Teixeira, W., Tassinari, C.C.G., Basei, M.A.S., 2000. Crustal evolution of the South American platform, in: Cordani, U.G., Milani, E.J., Thomaz Filho, A., Campos, D.A. (Eds.), Tectonic evolution of South America. International Geological Congress: Brazilian Academy of Science, 19-40, Río de Janeiro.

Dalla Salda, L.H., 1981. Tandilia, un ejemplo de tectónica de transcurrencia en basamento. Revista de la Asociación Geológica Argentina 2, 204-207.

Dalla Salda, L.H., Franzese, J.R., 1989. Los granitoides de Tandil. Primeras Jornadas Geológicas Bonaerenses, Actas 1, 845-861, Buenos Aires.

Dalla Salda, L.H., Iñiguez, A.M., 1979. La Tinta, Precámbrico y Paleozoico de Buenos Aires. 7° Congreso Geológico Argentino, Actas 1, 539-550, Neuquén.

Dalla Salda, L.H., Bossi, J., Cingolani, C.A., 1988. The Río de la Plata cratonic region of southwestern Gondwana. Episodes 11, 263-269.

Dalla Salda, L.H., de BarRío, R.E., Echeveste, H.J., Fernández, R.R., 2005. El basamento de las Sierras de Tandilia, in: de Barrio, R.E., Etcheverry, R.O., Caballé, M.F., Llambías, E. (Eds.), Geología y Recursos Minerales de la Provincia de Buenos Aires. Relatorio del 16° Congreso Geológico Argentino, 31-50, La Plata.

Delpino, S.H., 2000. Evolución metamórfica del sector nororiental del basamento de Tandilia, Argentina: metamorfismo en facies granulita y anatexis cortical. Doctoral Thesis, Universidad Nacional del Sur, 180p., Bahía Blanca.

Delpino, S.H., Dristas, J.A., 2008. Dolomitic marbles and associated calc-silicates, Tandilia belt, Argentina: Geothermobarometry, metamorphic evolution, and P-T path. Journal of South American Earth Sciences 23, 147-175.

Droop, G.T.R., 1987. A general equation for estimating Fe□3+ concentrations in ferromagnesian silicates and oxides from microprobe analyses, using stoichiometric criteria. Mineralogical Magazine 51, 431-435.

Farquhar, J.H., Wing, B.A., 2003. Multiple sulfur isotopes and the evolution of the atmosphere. Earth Planetary Science Letters 213, 1-13.

Favetto, A., Rocha, V., Pomposiello, C., García, R., Barcelona, H., 2015. A new limit for the NW Río de la Plata Craton border at about 24°S (Argentina) detected by Magnetotellurics. Geologica Acta 13, 243-254.

Frisicale, M.C., Dimieri, L.V., Dristas, J.A., 1999. Megacizalla en Boca de la Sierra, Tandilia: Convergencia normal? 14° Congreso Geológico Argentino Actas 1, 168-171, Salta.

Fulfaro, V.J., 1996. Geología del Paraguay Oriental, in: Comin-Chiaramonti, P., Gomes, C.B. (Eds.), Alkaline magmatism in central-eastern Paraguay: São Pablo, Edusp/Fapesp, 17-29.

Fuck, R.A., Neves, B:B:B., Schobbenhaus, C., 2008. Rodinia descendants in South America. Precambrian Research ,160, 108-126.

Gaucher, C., Finney, S.C., Poiré, D.G., Valencia, V.A., Grove, M., Blanco, G., Pamoukaghlián, K.,Gómez Peral, L. 2008. Detrital zircon ages of Neoproterozoic sedimentary successions in Uruguay and Argentina: insights into the geological evolution of the Río de la Plata Craton. Precambrian Research 167, 150-170.

Gaucher, C., Bossi, J., Blanco, G. , 2009. Palaeogeography. Neoproterozoic-Cambrian evolution of the Río de la Plata Palaeocontinent, in Gaucher, C., Sial, A.N., Halverson, G.P., and Frimmel, H.E., (Eds.), Neoproterozoic-Cambrian Tectonics, Global Change and Evolution: A Focus on Southwestern Gondwana. Elsevier, Netherlands, Developments in Precambrian Geology 16, 131-141.

Gaucher, C., Frei, R., Chemale, F., Frei, D., Bossi, G., Martinez, G., Chiglino, L., Cernuschi, F., 2011. Mesoproterozoic evolution of the Río de la Plata Craton in Uruguay: at the heart of Rodinia? International Journal of Earth Sciences 100, 2-3.

Gauthier-Lafaye, F., Weber, F., 1989. The Francevillian (Lower Proterozoioc) uranium ore deposits of Gabon. Economic Geology 84, 2267-2285.

Gioia, S.M.C.L., Pimentel, M.M., 2000. The Sm-Nd isotopic method in the geochronology laboratory of the University of Brasília. Anais da Academia Brasileira de Ciências 72, 219-245.

Goldstein, S.L., Arndt, N.T., Stallard, R.F., 1997. The history of a continent from U-Pb ages of zircons from Orinoco River sand and Sm-Nd isotopes in Orinoco basin river sediments. Chemical Geology 139, 269-284.

Gómez Peral, L.E., 2008. Petrología y diagénesis de las unidades sedimentarias precámbricas de Olavarría, Provincia de Buenos Aires. Doctoral Thesis, Universidad Nacional de La Plata, 619 p., La Plata.

Gómez Peral, L.E., Poiré, D.G., Canalicchio, J.M., 2005. Clastos fosfáticos en la Formación Villa Mónica, Neoproterozoico infeRíor, Sistema de Tandilia, Argentina. 16° Congreso Geológico Argentino Actas 3, 125-132, La Plata

Gómez Peral, L.E, Poiré, D.G., Strauss, H., Zimmermann, U., 2007. C-O Isotope data and diagenetic constraints of the Neoproterozoic Sierras Bayas Group, (SW Gondwana), Argentina. Chemical Geology 237, 127-146.

Halpern, M., Umpierre Urquhart, M., Linares, E., 1970. Radiometric ages of crystalline rocks from southern South America, as relate to Gondwana and Andean geologic provinces. 4th Upper Mantle Symposium, Petrología y Volcanismo, 345-356, Buenos Aires.

Hart, S.R., Krogh, T.E., Davis, G.L., Aldrich, L.T., Minizaga, R., 1965. A geochronological approach to the continental drift hypothesis. Carnegie Institute Whashington Yearbook 65, 57-59.

Hartmann, L.A., Piñeyro, D., Bossi, J., Leite, J.A.D., McNaughton, N.J., 2000a. Zircon U-Pb SHRIMP dating of Paleoproterozoic Isla Mala granitic magmatism in the Río de la Plata Craton, Uruguay. Journal of South American Earth Sciences 13, 105-113.

Hartmann, L.A., Santos, J.O.S, McNaughton, N.J., Vaconcellos, M.A.Z., Silva, L.C., 2000b. Ion microprobe (SHRIMP) dates complex granulite from Santa Catarina, southern Brazil. Anais Da Academia Brasilera De Ciências 72, 559-572.

Hartmann, L.A., Santos, J.O.S., Bossi, J., Campal, N., Schipilov, A., McNaughton, N.J. 2002a. Zircon and titanite U-Pb SHRIMP geochronology of Neoproterozoic felsic magmatism on the eastern border of the Río de la Plata Craton, Uruguay. Journal of South American Earth Sciences 15, 229-236.

Hartmann, L.A., Santos, J.O.S., Cingolani, C.A., McNaughton, N.J., 2002b. Two Paleoproterozoic Orogenies in the Evolution of the Tandilia Belt, Buenos Aires, as evidenced by zircon U-Pb SHRIMP geochronology. International Geology Review 44, 528-543.

Hartmann, L.A., Chemale, F.Jr., Philipp, R.P., 2007. Evolucão Geotectônica do Río Grande do Sul no Pré-Cambriano, in: Ianuzzi, R., Frantz, J.C. (Eds.), 50 anos de Geologia do Río Grande do Sul. Instituto de Geociências. Contribuições 1, 97-123, Porto Alegre, Brazil.

Holland, H.D., 1994. Early Proterozoic atmospheric changes, in: Bengstone, S. (Ed.), Early Life on Earth. Nobel Symposium, 84. Columbia University Press, 237-344.

Holland, H.D., 2002. Volcanic gases, black smokers, and the Great Oxidation Event. Geochimica et Cosmochemica 66, 3811-3826.

Iñiguez, A.M., Zalba, P., 1974. Nuevo nivel de arcillas en la zona de Cerro Negro, partido de Olavarría, provincia de Buenos Aires. Anales del Lemit 264, 95-100.

Isley, A.E., Abbott, D.H., 1999. Plume-related mafic volcanism and the deposition of banded iron formation. Journal of Geophysical Research of Solid Earth 104, 15461-15477.

Karhu, J.A., 1993. Palaeoproterozoic evolution of the carbon isotope ratios of sedimentary carbonates in the Fennos-candian Shield. Geological Survey of Finland bulletin 371, 1-87.

Karhu, J.A., Holland, H.D., 1996. Carbon isotopes and rise of the atmospheric oxygen. Geology 2, 6-9.

Kretz, R., 1983. Symbols for rock-forming minerals. American Mineralogist 68, 277-279.

Lajoinie, M.F., 2015. Geología y Geoquímica del skarn San Miguel, Sistema de Tandilia, provincia de Buenos Aires. Doctoral Thesis, Universidad Nacional de La Plata, 300p., La Plata.

Lajoinie, M.F., Lanfranchini, M.E., Etcheverry, R.O., Recio, C., 2013. Zonación mineral vinculada a procesos geoquímicos en el skarn San Miguel, Sierras SeptentRíonales de la provincia de Buenos Aires. Revista de la Asociación Geológica Argentina 70, 402-412.

Lajoinie, M.F., Etcheverry, R.O., Lanfranchini, M.E., Cabana, C., 2014a. Geología, geoquímica y génesis de diques proterozoicos del área de San Miguel, Sierras SeptentRíonales de la provincia de Buenos Aires. Revista de la Asociación Geológica Argentina, 71: 404-415.

Lajoinie, M.F., Lanfranchini, M.E., Etcheverry, R.O. Recio, C., 2014b. Primeros registros del "Evento Lomagundi-Jatuli" en mármoles del basamento de las Sierras Septentrionales de la provincia de Buenos Aires, Cratón del Río de la Plata. Revista de la Asociación Geológica Argentina 71, 585-597.

Lajoinie, M.F., Lanfranchini, M.E., Etcheverry, R.O., Benítez, M.E., de la Cal, H.G., 2017. Estudios geoquímicos de Tierras Raras e ytrio en rocas de la Formación El Cortijo, Sierras

SeptentRíonales de la provincia de Buenos Aires. 20° Congreso Geológico Argentino, 33-34. San Miguel de Tucumán.

Linares, E., González, R.R., 1990. Catálogo de edades radimétricas de la República Argentina. Revista de la Asociación Geológica Argentina, Publicaciones Especiales 19, 1957-1987.

Lindsay, J.F., Brasier, M.D., 2002. Did global tectonics drive early biosphere evolution? Carbon isotope record from 2.6 to 1.9 Ga carbonates of Western Australian basins. Precambrian Research 114, 1-34.

Maheshwari, A., Sial, A.N., Chittora, V.K., 1999. High δ^{13}C Paleoproterozoic carbonates from the Aravalli Supergroup, Western India. International Geology Review 41, 949-954.

Maheshwari, A., Sial, A.N., Chittora, V.K., Harsh, B., 2002. A positive $\delta^{13}C_{carb}$ anomaly in Paleoproterozoic carbonates of Aravalli Craton,Western India: "Support for a global isotopic excursion". Journal Asian Earth Science 21, 59-67.

Maheshwari, A., Sial, A.N., Gaucher, C., Bossi, J., Bekker, A., Ferreira, V.P., Romano, A.W., 2010. Global nature of the Paleoproterozoic Lomagundi carbon isotope excursion: A review of occurrences in Brazil, India, and Uruguay. Precambrian Research 182, 274-299.

Marchese, H.G., Di Paola, E., 1975. Miogeosinclinal Tandil. Revista de la Asociación Geológica Argentina 30, 161-179.

Martin, A.P., Condon, S.J., Prave, A.R., Lepland, A., 2013. A review of temporal constraints for the Palaeoproterozoic large, positive carbonate isotope excusion (the Lomagundi-Jatuli Event). Earth Science Reviews 127, 242-261.

Master, S., Verhagen, B.T., Duane, M.J., 1990. Isotopic signatures of continental and marine carbonates from the Magondi Belt, Zimbabwe: Implications for the global carbon cycle at 2.0 Ga. 23rd Earth Science Congress of Geological Society of South Africa, Abstracts, 346-348, Cape Town.

Master, S., Bekker, A., Hofmann, A., 2010. A review of the stratigraphy and geological setting of the Plaeoproterozoic Magoni Supergroup, Zimbabwe - Type locality for the Lomagundi carbon isotope excursion. Precambrian Research 182, 254-273.

Melezhik, V.A., Fallick, A.E., 1996. A widespread positive $\delta^{13}C_{carb}$ anomaly at around 2.33-2.06 Ga on the Fennoscandian Shield: a paradox? Terra Nova 8, 141-285.

Melezhik, V.A., Fallick, A.E., Clark, T., 1997. Two billion year old isotopically heavy carbon: evidence from the Labrador Trough, Canada. Canadian Journal of Earth Science 34, 272-285.

Melezhik, V.A., Fallick, A.E., 2010. On the Lomagundi-Jatuli carbon isotopic event: evidence from the Kalix Greenstone Belt, Sweden. Precambrian Research 179, 165-190.

Melezhik, V.A., Fallick, A.E., Medvedev, P.V., Makarikhin, V.V., 1999. Extreme $^{13}C_{carb}$ enrichment in ca.2.0 Ga magnesite-stromatolite-dolomite-'red beds' association in a global context: a case for the worl dwide signal enhanced by a local environment. Earth-Science Reviews 48, 71-120.

Melezhik, V.A., Gorokhov, I.M., Fallick, A.E., Gjelle, S. 2001. Strontium and carbon isotope geochemistry applied to dating of carbonate sedimentation: an example from high-grade rocks of the Norwegian Caledonides. Precambrian Research 108: 267-292.

33

Melezhik, V.A., Fallick, A.E., Kuznetsov, A.B., 2005. Palaeoproterozoic, rift-related, ^{13}C-rich, lacustrine carbonates, NW Russia-Part 2: Global isotope signal recorded in the lacustrine dolostones. Transactions of the Royal Society of Edinburgh Earth Science 95, 423-444.

Melezhik, V.A., Huhma, H., Condon, D.J., Fallick, A.E., Whitehouse, M.J., 2007. Temporal constraints on the Paleoproterozoic Lomagundi- Jatuli carbon isotopic event. Geology 35, 655-658.

Mirota, M.D., Veizer, J., 1994. Geochemistry of Precambrian Carbonates. Aphebian Albanel Formations, Quebec, Canada. Geochimica et Cosmochimica Acta 58, 1735-1745.

Nosaki, Y., Zhang, J., Amakawa, H., 1997. The fractionation between Y ans Ho in the marine environment. Earth and Planetary Science Letters 148, 329-340.

Oyhantçabal, P., Bettucci, L.S., Pecoits, E., Aubet, N., Peel, E., Preciozzi, F., Basei, M.A.S., 2005. Nueva propuesta estratigráfica par alas supracorticales del Cinturón Dom Feliciano (Proterozoico, Uruguay), 12° Congreso Latinoamericano de Geología, Ministerio de Energía y Minas de Ecuador, Quito (CD-ROM).

Oyhantçabal, P., Siegesmund, S., Wemmer, K., 2010. The Sierra Ballena shear zone in the southernmost Dom Feliciano Belt (Uruguay): Evolution, kinematics, and deformation conditions. International Journal of Earth Sciences 99, 1227-1246.

Oyhantçabal, P., Siegesmund, S., Wemmer, K., 2011. The Río de la Plata Craton: A review of units, boundaries, ages and isotopic signatures. International Journal of Earth Science 100, 201-220.

34

Pankhurst, R.B., Ramos, V.A., Linares, E., 2003. Antiquity of the Río de la Plata Craton in Tandilia, southern Buenos Aires province, Argentina. Journal of South American Earth Sciences 16, 5-13.

Pimentel, M.M., Fuck, R.A., 1992. Neoproterozoic crustal accretion in central Brazil. Geology 20, 375-379.

Poiré, D.G., 1987. Mineralogía y sedimentología de la Formación Sierras Bayas en el Núcleo SeptentRíonal de las sierras homónimas, partido de Olavarría, provincia de Buenos Aires. Doctoral Thesis, Universidad Nacional de La Plata, 271 p., La Plata.

Poiré, D.G., 1993. Estratigrafía del Precámbrico sedimentaRío de Olavarría, Sierras Bayas, provincia de Buenos Aires, Argentina. 10° Congreso Geológico Argentino y 3° Congreso de Exploración de Hidrocarburos, Actas 2, 1-11, Mendoza.

Poiré, D.G., del Valle, A., Regalía, G.M., 1984. Trazas fósiles en cuarcitas de la Formación Sierras Bayas (Precámbrico) y su comparación con las de la Formación Balcarce (Cambro-Ordovícico), Sierras SeptentRíonales de la provincia de Buenos Aires. 9° Congreso Geológico Argentino, Actas 4, 249-266, Río Negro.

Poiré, D.G., Spalletti, L.A, del Valle, A., 2003. The Cambrian-Ordovician siliciclastic platform of the Balcarce Formation (Tandilia System, Argentina): facies, trace fossils, palaeoenvironments and sequence stratigraphy. Geologica Acta 1, 41-60.

Quartino, B., Villar Fabre, J., 1967. Geología y petrología del basamento de Tandil y Barker, provincia de Buenos Aires, a la luz del estudio de localidades críticas. Revista de la Asociación Geológica Argentina 22, 223-251.

Ramos, A., 1985. Interpretación geológica preliminar de edades radimétricas en la Sierra del Tigre, Tandil, provincia de Buenos Aires. In: 1° Jornadas Geológicas Bonaerense, La Plata, Resúmenes, p. 125.

Ramos, V.A., 1988. Late Proterozoic - Early Paleozoic of South America: A collisional history. Episodes 11, 168-174.

Ramos, V.A., 1999. Evolución tectónica del territoRío argentino, in: Caminos, R. (Ed.), Geología Argentina. Anales SEGEMAR 24, 715-784, Buenos Aires.

Ramos, V., Vujovich, G., Martino, R., Otamendi, J., 2010. Pampia: A large cratonic block missing in the Rodinia supercontinent. Journal of Geodynamics 50, 243-255.

Rapela, C.W., Pankhurst, R. J., Casquet, C., Fanning, C.M., Baldo, E.G., González-Casado, J.M., Galindo, C., Dahlquist, J., 2007. The Río de la Plata Craton and the assembly of SW Gondwana. Earth Science Reviews 83, 49-82.

Rapela, C.W., Fanning, C.M., Casquet, C., Pankhurst, R.J., Spalletti, L., Pain, D., Baldo, G.E., 2011. The Río de la Plata Craton and the adjoining Pan-African/Brasiliano terranes: Their origins and incorporation into south-west Gondwana. Gondwana Research 20, 673-690.

Reinhard, C.T., Planavsky, N.J., Lyons, T.W., 2013. Long-term sedimentary recycling of rare sulphur isotope anomalies. Nature 497, 100-103.

36

Santos, J.O.S., Hartmann, L.A., Bossi, J., Campal, N., Schipilov, A., Piñeiro, McNaughton, J., 2003. Duration of the Trans-Amazonian Cycle and its correlation within South America based on U-Pb SHRIMP geochronology of the La Plata craton, Uruguay. International Geology Review 45, 27-48.

Santos, J.O.S, Chernicoff, C.J., Zappettini, E.O., Naughton, N.J., Hartmann, L.A., 2017. Large geographic and temporal extensions of the Río de la Plata Craton, South America, and its metacratonic eastern margin. International Geology Review, 1-30. doi: 10.1080/00206814.2017.1405747

Schidlowski, M., Eichmann, R., Junge, C.E., 1975. Precambrian sedimentary carbonates: carbon and oxygen isotope geochemistry and implications for the terrestrial oxygen budget. Precambrian Research 2, 1-69.

Schidlowski, M., Eichmann, R., Junge, C.E., 1976. Carbon isotope geochemintry of the Precambrian Lomagundi carbonate province, Rhodesia. Geochemical et Cosmochemical Acta 40, 449-455.

Schidlowski, M., Hayes, J.M., Kaplan, I.R., 1983. Isotopic inferences of ancient biochemistries: carbon, hydrogen and nitrogen, in: Schopf, J.W. (Ed.), Earth's Earliest Biosphere: Its Origin and Evolution. Princeton University Press, 149-186, Princeton.

Schröder, S., Bekker, A., Beukes, N.J., Strauss, H., van Niekerk, H.S., 2008. Rise in seawater: sulphate concentration associated with the Paleoproterozoic positive carbon isotope excursion evidence from sulphate evaporates in the ~2.2-2.1 Gyr shallow marine Lucknow Formation South Africa. Terra Nova 20, 108-117.

Seilacher, A., Cingolani, C.A., Varela, R., 2002. Ichnostratigraphic correlation of Early Paleozoic sandstones in North Africa and Central Argentina, in: Salem, M., Oun, K. (Eds.), Geology of Northwest Libya, volume 1. Earth Science Society of Lybia, 275-292.

Shieh, Y.N., Taylor, H.P., 1969. Oxygen and hydrogen isotope studies of contact metamorphism in the Santa Rosa Range, Nevada and other areas. Contributions to Mineralogy and Petrology 20, 306-356.

Shields, G.A., Veizer, J., 2002. The Precambrian marine carbonate isotope database: version 1.1. Geochemistry Geophysics Geosystems, 3.

Siga Júnior, O., Basei, M.A.S., Passarelli, C.R., Harara, O.M., Sato, K., Cury, L.F., Prazeres Filho, H.C., 2007. Geocronologia de rochas gnáissico-migmatíticas e sienograníticas do Núcleo Setuva (Pr): Implicaões tectônicas. Revista Brasileira de Geociências 37, 114-128.

Tang, H., Chen, Y., Wu, G., Lai, Y., 2011. Paleoproterozoic positive $\delta^{13}C_{carb}$ excursion in the northeastern Sino-Korean craton: Evidence of the Lomagundi Event. Gondwana Reasearch 19, 471-481.

Taylor, S.R., MacLennan, S.M., 1985. The Continental Crust: Its Composition and Evolution. Blackwell, Oxford, p. 312.

Teruggi, M.E., Mauriño, V.E., Limousin, T.A., Schauer, O., 1958. Geología de las Sierras de Tandil. Revista de la Asociación Geológica Argentina 13, 185-204.

Teruggi, M.E., Kilmurray, J.O., 1975. Tandilia. 6° Congreso Geológico Argentino, RelatoRío Geología de la provincia de Buenos Aires, 55-77.

Teruggi, M.E., Kilmurray, J.O., 1980. Sierras SeptentRíonales de la provincia de Buenos Aires. Geología Regional Argentina. Academia Nacional de Ciencias 2, 919-956, Córdoba.

Teruggi, M.E., Leguizamón, M.A., Ramos, V.A., 1988. Metamorfitas de bajo grado con afinidades oceánicas en el basamento de Tandil: su implicancia geotectónica, provincia de Buenos Aires. Revista de la Asociación Geológica Argentina 43, 366-374.

Tohver, E., Cawood, P.A., Rosselo, E.A., Jourdan, F., 2012. Closure of the Clymene Ocean and formation of West Gondwana in the Cambrian: evidence from the Sierras Australes of the southernmost Río de la Plata Craton, Argentina. Gondwana Research 21: 394-405.

Valley, J.W., 1986. Stable isotope geochemistry in metamorphic rocks, in: Valley, J.W., Taylor, H.P. y O'Neil, J.R. (Eds.), Stable Isotopes in High Temperature Geological Processes, MSA. Reviews in Mineralogy 16, 445-490, Washington.

Villar Fabre, J.F., 1954. Resumen geológico de la hoja 32q, Sierras de Tandil. Revista de la Asociación Geológica Argentina, 9, 109-130.

Young, G.M., Long, D.G.F., Fedo, C.M., Nesbitt, H. W., 2001. Paleoproterozoic Huronian basin: product of a Wilson cycle punctuated by glaciations and a meteorite impact. Sedimentary Geology 141, 233-250.

Zheng, Y.F., 1993. Calculation of oxygen isotope fractionation in anhydrous silicate minerals. Geochemica et Cosmochemica Acta 57, 1079-1091.

Zimmermann, U., Spalletti, L.A., 2009. Provenance of the Lower Palaeozoic Balcarce Formation (Tandilia System, Buenos Aires province, Argentina): implications for palaeogeographic reconstructions of SW Gondwana. Sedimentary Geology 219, 7-23.

Figure 1: Worldwide distribution of the Lomagundi-Jatuli event carbonates (modified from Melezhik *et al.*, 1999; Tang *et al.*, 2011) and San Miguel marble location (Tandilia System, Río de la Plata Craton).

Figure 2: a) Location, extension, and shape of the Río de la Plata Craton proposed by different authors as follows: (A) Santos *et al*. (2017), (B) Bossi and Cingolani (2009), (C) Rapela *et al*. (2007), (D) Fuck *et al*. (2008), (E) Oyhantçabal *et al*. (2011) and Rapela *et al*. (2011), (F) Ramos *et al*. (2010). P-terrane: Patagonian terrane b) Schematic geological map of the RPC outcrops in Brazil Paraguay, Argentina, and Uruguay, along with the Neoproterozoic terranes, belts, and major shear zones (modified from Santos *et al*., 2017). SYSZ: Sarandi del Yí Shear Zone, SBSZ: Sierra Ballena Shear Zone (Oyhantçabal *et al*., 2010a), R: Rivera, T: Tacuarembó, LA: Luís Alves, Ca: Camboriú, Cu: Curitiba, Sg: Sao Gabriel arc. BA-PA correspond to Buenos Aires-Piedra Alta terrane (Chernicoff *et al*., 2014). c) Geological map of the Tandilia System (Dalla Salda *et al*., 2005), the study area is highlighted (more detail in Fig. 4).

Figure 3: Schematic diagrams of the interpreted tectonic evolution for the Tandilia System (from Cingolani, 2010; Chernicoff *et al*., 2014): a) rift system initiation; b) beginning of subduction (after Teruggi *et al*., 1988; Ramos, 1999); and c) main collisions, crust thickening, transcurrent faults, anatexis.

Figure 4: Geological map of the study area. Modified from Lajoinie *et al.* (2014b).

Figure 5: a) Biotite gneiss outcrops. b) Detail of the gneiss banded structure, LG = leucocratic gneiss, MG = melanocratic gneiss. c) Migmatite with stromatic structure outcrop. d) Detail of garnet-leucosome in contact with the gneiss.

Figure 6: a) Marble outcrop cut by leucosome intrusions. b) Schematisation of the leucosome-marble outcropping relationships. c) Detail of the marble lenses and the leucosome intrusions. d) Wollastonite-vesuvianite-grossular-diopside skarn. Mineral abbreviations according to Kretz (1983).

Figure 7: Sample locations. a) Cross-section in the marble from the furthest to the nearest sectors to the contact with leucogranite bodies. b) Cross-section between two leucogranite intrusions.

Figure 8: SM marble microscopy aspect. a) Prismatic and basal sections of diopside crystal surrounded by calcite. b) Intracrystalline deformation evidence of tapered and deformed lamellae twins in calcite, and undulose extinction in quartz. c) Two types of mechanical twining: crossing (CT) and stopping (ST). d) Diopside crystal replacements by tremolite and chlorite. Also, more evidence of deformation as undulose extinction (UE) and tapered twins in calcite are shown. Mineral abbreviations according to Kretz (1983).

Figure 7: Sample locations. a) Cross-section in the marble from the furthest to the nearest sectors to the contact with leucogranites bodies. b) Cross-section between two leucogranite intrusions.
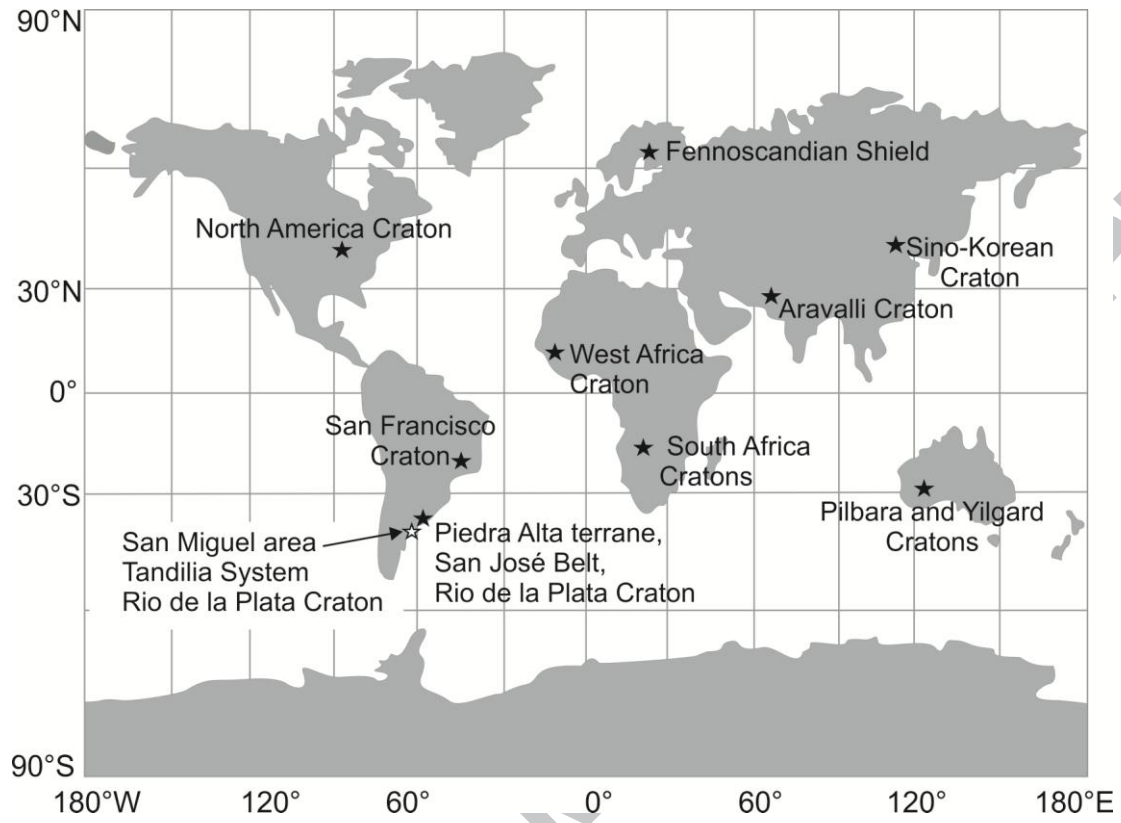
Figure 8: SM marble microscopy aspect. a) Prismatic and basal sections of diopside crystal surrounded by calcite. b) Intracrystalline deformation evidence of tapered and deformed lamellae twins in calcite, and undulose extinction in quartz. c) Two types of mechanical twinning: crossing (CT) and stopping (ST). d) Diopside crystal replacements by tremolite and chlorite. Also, more evidence of deformation as undulose extinction (UE) and tapered twins in calcite are shown. Mineral abbreviations according to Kretz (1983).

Figure 9: Geochemical binary diagram (marble samples): a) CaO vs. Sr; b) $\sum$REE vs. Al_2O_3; and c) Ti_2O vs. Zr. The first diagram shows a slightly negative relation, while the other two exhibit positive correlations.

Figure 10: Post-Archaean Average Australian Shale (PAAS; Taylor and McLennan, 1985) normalised rare earth elements and yttrium data from SM marble.

Figure 11: $\delta^{18}O$ *vs*. $\delta^{13}C$ values of the calcite crystals from the SM marble. The boxes correspond to typical values of: Lomagundi-Jatuli carbonates (LJC, Martin *et al.*, 2013), normal marine carbonates (NMC), and igneous calcites (IC), according to Bowman (1988).

Figure 12: Important events during the Archaean-Palaeoproterozoic transition (Martin *et al.*, 2013). a) Rise in oxygen levels between 2.45 and 2.20 Ga. %P.A.L.: present atmospheric levels. Reducing (dark boxes) and oxidising (grey boxes) atmospheres are plotted (Holland, 1994; Bekker and Holland, 2012). b) Distribution of Fe deposits (Isley and Abbott, 1999). $\Delta^{33}S$ values according to Farquhar and Wing (2003) and Reinhard *et al.* (2013). c) $\delta^{13}C$ from marine carbonates (Shields and Veizer, 2002). Also, SM marble is plotted.

c) LATE RHYACIAN

COLLISION, CRUST THICKENING, TRANSCURRENT FAULTS AND ANATEXIS.

2.2-2.0 Ga

calc-alkaline magmatism

NW

SE

Partial melting (Leucogranites)

b) EARLY RHYACIAN

SUBDUCTION

2.37-2.2 Ga

EL CORTIJO ISLAND ARC

TANDILIA TERRANE

NW

SE

BA-PA TERRANE

a) SIDEARIAN

RIFT SYSTEM

2.37 Ga

NW

SE

BA-PA TERRANE

TANDILIA TERRANE
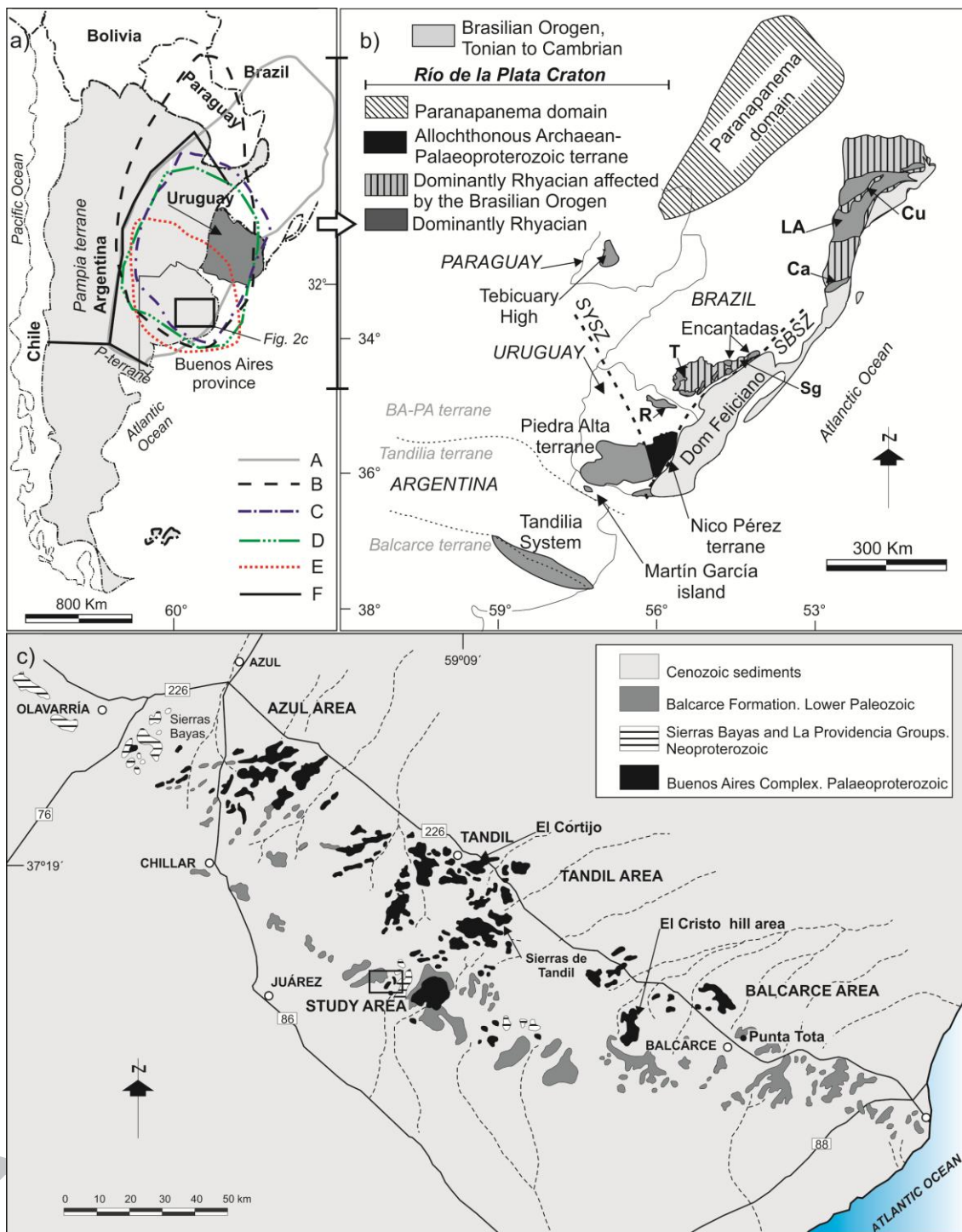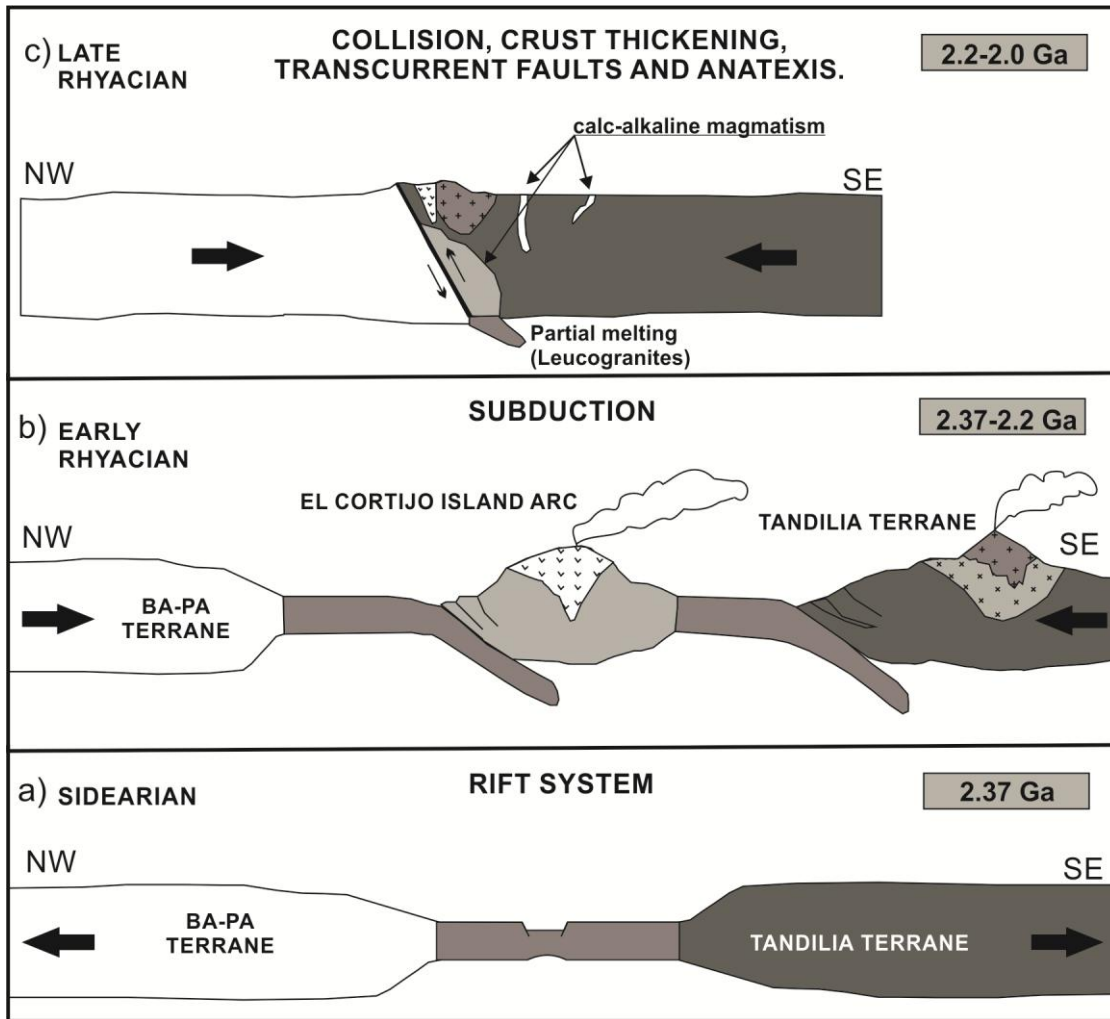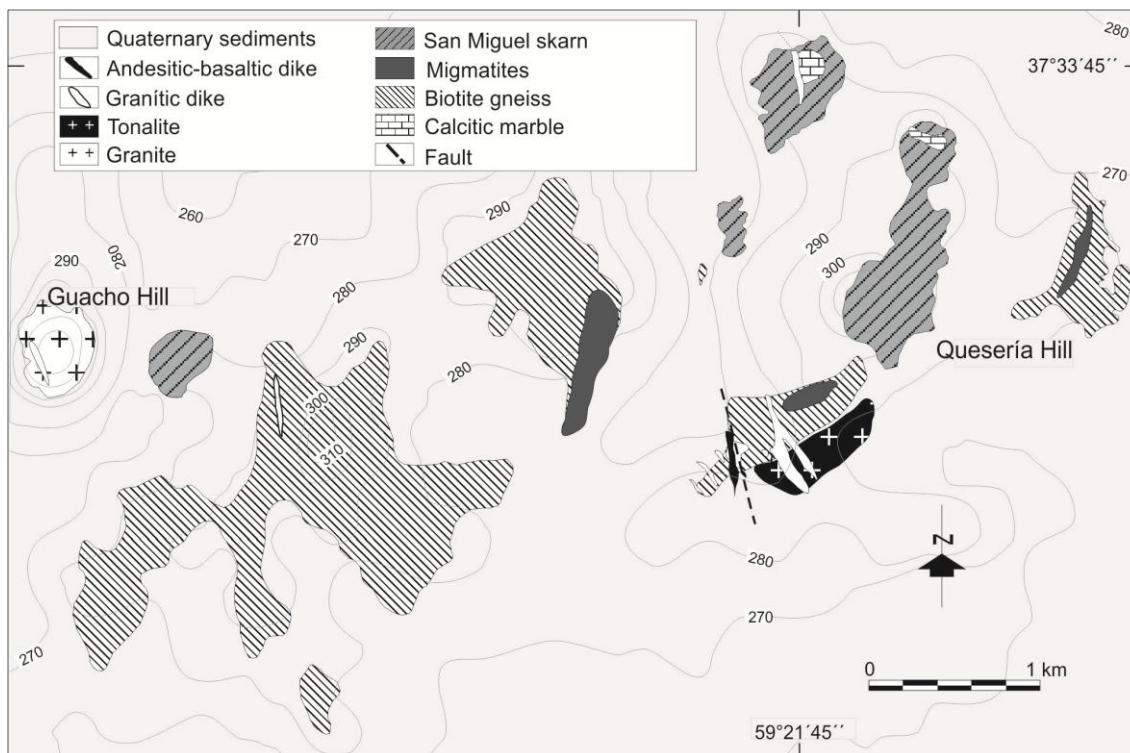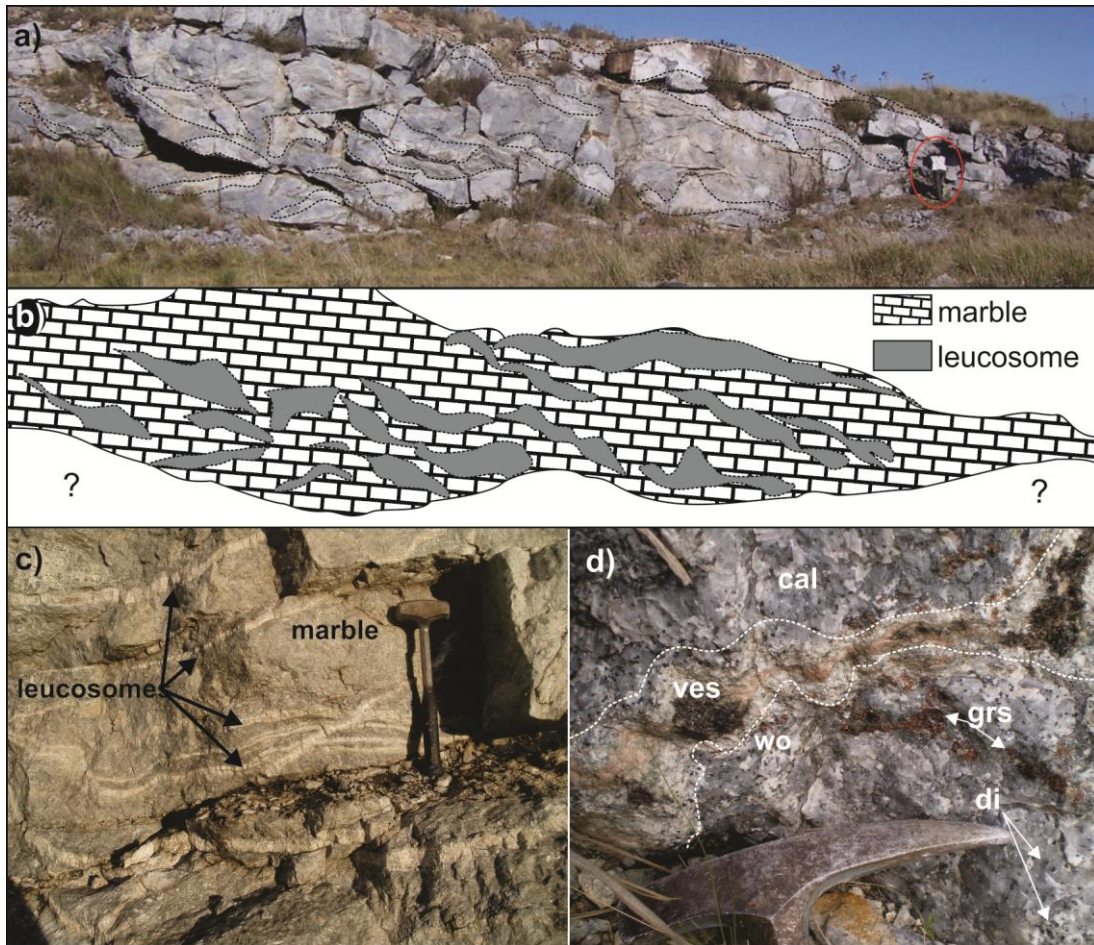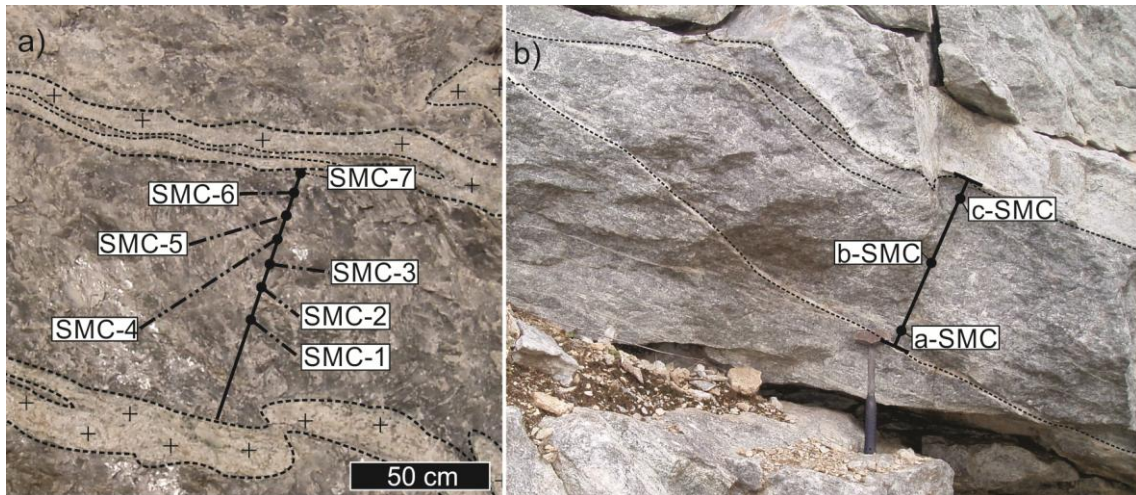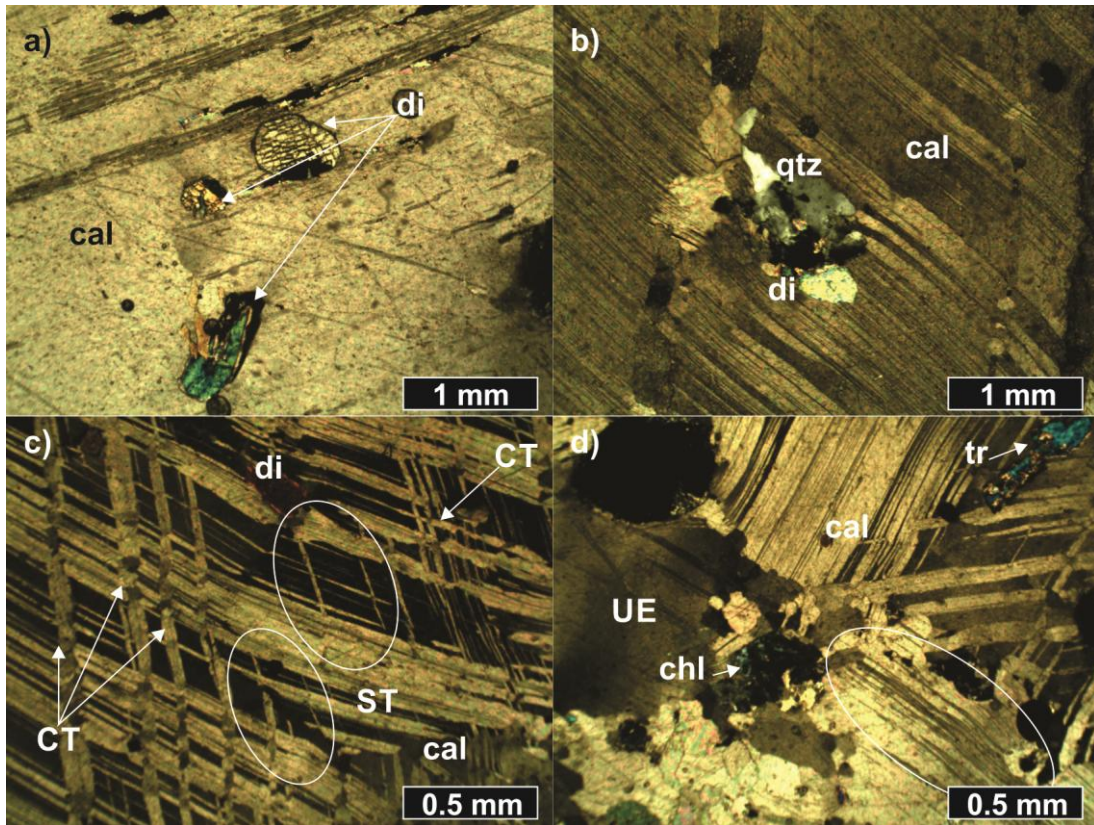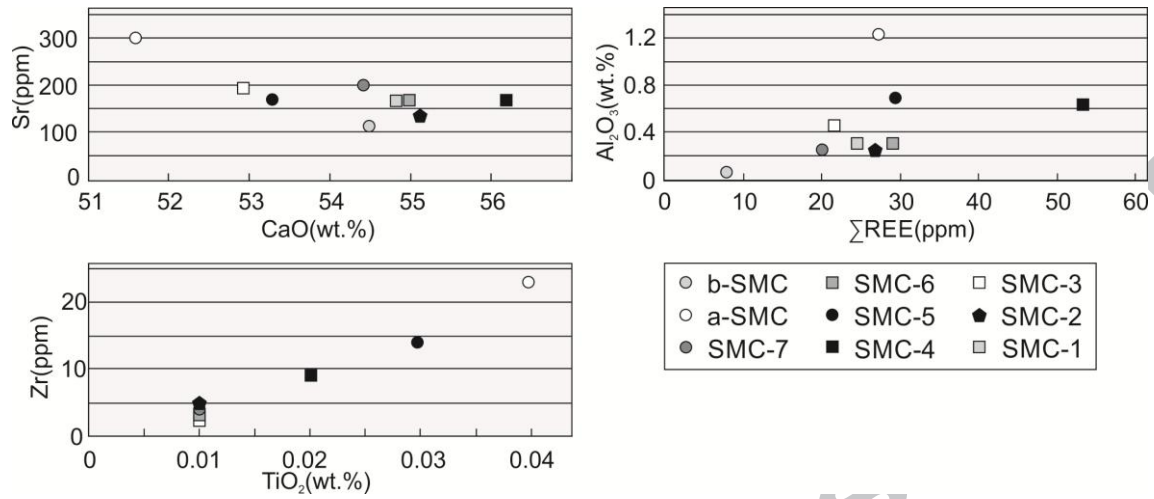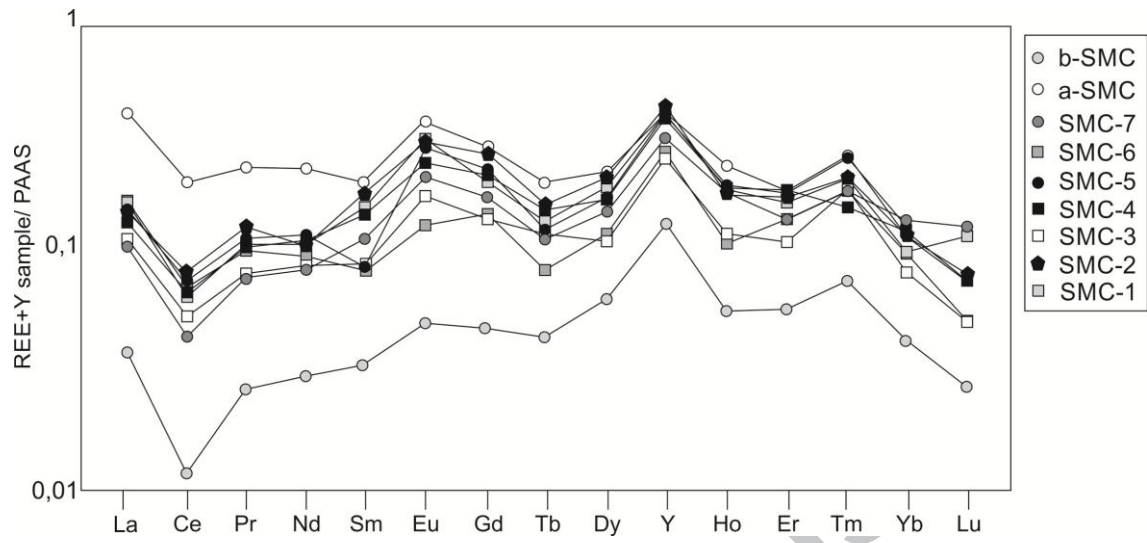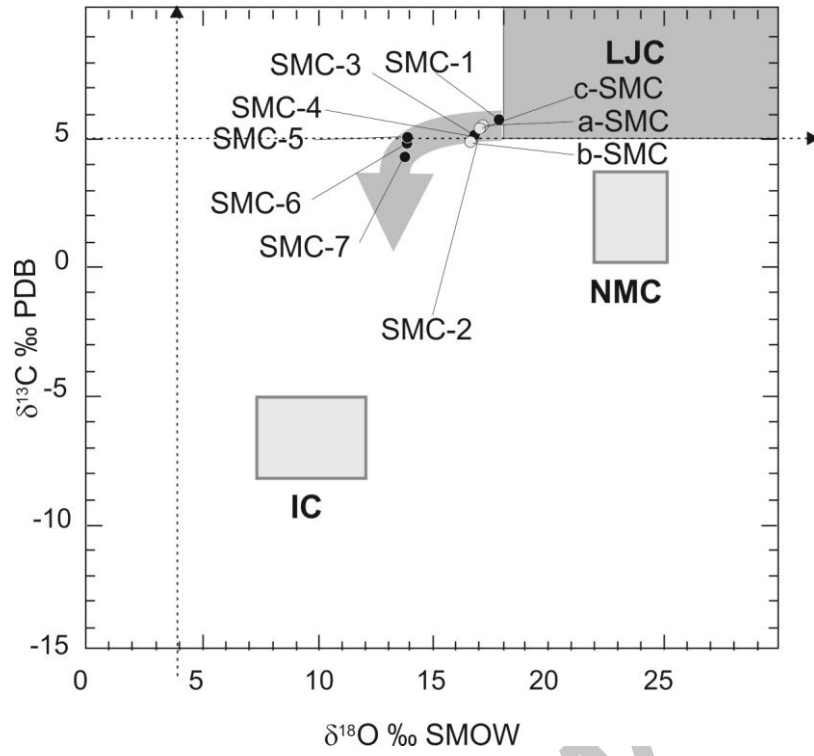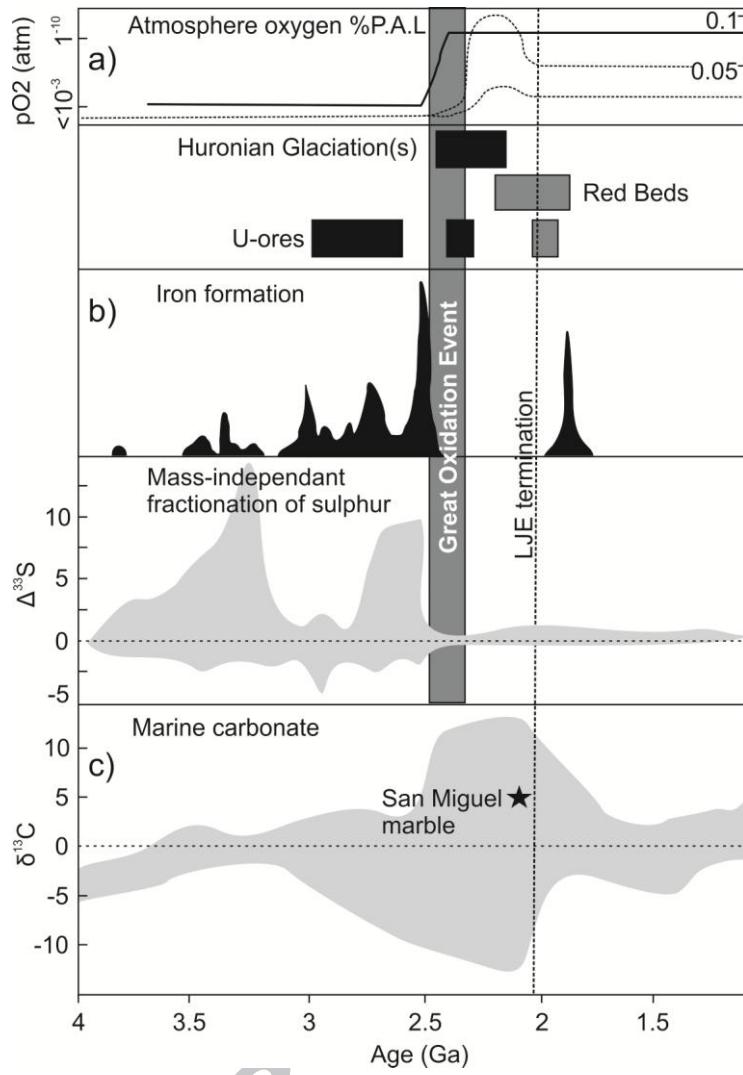
Table 1: Representative electron microprobe analyses of clinopyroxene crystals from SM marble.

	P1	P2	P3	P4	P5	P6	P7	P8
				clinopyroxene composition				
wt.%								
SiO_2	52.82	53.87	53.12	53.16	53.25	52.05	52.63	53.08
TiO_2	0.00	0.02	0.04	0.00	0.04	0.07	0.00	0.02
Al_2O_3	0.63	0.53	0.63	0.7	0.66	0.31	0.63	0.17
Cr_2O_3	0.01	0.04	0.03	0.02	0	0	0	0.03
FeO*	6.99	5.39	5.48	6.62	5.37	10.93	8.65	8.79
Fe_2O_3*	1.71	1.15	1.68	1.65	1.43	0.76	1.66	0.93
MnO	0.01	0.05	0.04	0.06	0.02	0.08	0.00	0.04
MgO	12.85	14.25	13.84	13.16	14.02	10.89	11.63	12.39
NiO	0.03	0	0.07	0	0	0.06	0	0.01
CaO	25.34	25.65	25.74	25.7	25.59	24.78	25.76	25.61
Na_2O	0.21	0.19	0.16	0.17	0.18	0.09	0.18	0.08
K_2O	0.03	0.04	0.01	0	0	0.01	0.01	0.03
P_2O_5	0.16	0.17	0.14	0.11	0.18	0.17	0.14	0.21
$\sum$	100.79	101.35	100.97	101.35	100.74	100.2	101.28	101.38
cations				6 oxygens				
Si	1.96	1.97	1.96	1.96	1.97	1.98	1.96	1.97
P	0.00	0.00	0.00	0.00	0.00	0.00	0.00	0.00
Al	0.03	0.02	0.03	0.03	0.03	0.01	0.03	0.01
Fe^{+3}	0.01	0	0.01	0.01	0	0.01	0.01	0.02
$\sum$	2.00	2.00	2.00	2.00	2.00	2.00	2.00	2.00

Ti	0.00	0.00	0.00	0.00	0.00	0.00	0.00	0.00
Al	0.00	0.00	0.00	0.00	0.00	0.00	0.00	0.00
Cr	0.00	0.00	0.00	0.00	0.00	0.00	0.00	0.00
Fe^{+3}	0.05	0.03	0.04	0.04	0.04	0.02	0.05	0.02
Fe^{+2}	0.21	0.16	0.16	0.2	0.16	0.34	0.27	0.26
Mn	0.00	0.00	0.00	0.00	0.00	0.00	0.00	0.00
Mg	0.71	0.78	0.76	0.72	0.77	0.62	0.65	0.69
Ni	0.00	0.00	0.00	0.00	0.00	0.00	0.00	0.00
Na	0.02	0.01	0.01	0.01	0.01	0.01	0.01	0.01
K	0.00	0.00	0.00	0.00	0.00	0.00	0.00	0.00
Ca	1.01	1.01	1.02	1.02	1.01	1.01	1.03	1.02
∑	2.00	2.00	2.00	2.00	2.00	2.00	2.00	2.00
∑Total	4.00	4.00	4.00	4.00	4.00	4.00	4.00	4.00
Molecular %								
Di	72.76	79.6	77.77	74.1	78.85	62.32	67.08	69.46
Hd	27.21	20.23	22.12	25.71	21.08	37.43	32.92	30.4
Jo	0.03	0.17	0.12	0.19	0.08	0.25	0	0.14
∑	100	100	100	100	100	100	100	100

* Calculated following Droop (1987).

Table 2: Major, minor and trace element compositions for all the marble study samples.

Locality	San Miguel marble, Tandilla System								
Sample #	SMC-1	SMC-2	SMC-3	SMC-4	SMC-5	SMC-6	SMC-7	a-SMC	b-SMC
wt.%									
SiO_2	2.18	2.54	4.57	3.28	4.16	6.59	4.08	8.65	1.62
Al_2O_3	0.32	0.22	0.46	0.6	0.69	0.3	0.23	1.22	0.06
Fe_2O_{3total}	0.33	0.46	0.66	0.32	0.37	0.3	0.66	1.63	0.13
CaO	54.8	56.1	52.9	56.2	53.3	55	54.4	51.6	54.5
MgO	0.53	0.57	1.1	0.57	0.62	0.95	1.13	1.12	0.65
Na_2O	0.09	0.05	0.05	0.18	0.1	0.09	0.1	0.14	0.04
K_2O	0.04	0.05	0.01	0.05	0.02	0.03	0.02	0.03	0.01
TiO_2	0.01	0.01	0.01	0.02	0.03	<0.01	0.01	0.04	<0.01
MnO	0.01	0.01	0.01	0.01	0.01	0.01	0.01	0.03	0.01
P_2O_5	0.1	0.09	0.07	0.1	0.09	0.11	0.06	0.09	0.07
LOI	40.7	40.5	40.4	40.5	40.5	35.9	39.7	34.7	42.95
$\sum$	99.12	100.08	100.27	101.84	100.03	99.29	100.41	99.28	100.05
Ppm									
Ba	25.6	28.1	85.4	40.4	1080	22.1	21.1	37.1	10.4
Cr	10	<L.D	<L.D	10	<L.D	<L.D	<L.D	10	<L.D
Cs	0.07	0.08	0.02	0.03	0.07	0.02	0.02	0.09	0.03
Ga	1.4	1.3	0.6	2	0.8	1.3	1.7	2.8	<L.D
Hf	<0.2	<L.D	<L.D	0.2	0.3	<0.2	0.2	0.5	<L.D
Nb	0.4	0.6	0.4	0.8	0.4	0.4	0.3	1.1	0.3
Rb	0.6	0.3	<L.D	0.6	0.4	0.5	0.3	0.3	<L.D
Sn	<L.D	<L.D	<L.D	<L.D	<L.D	<L.D	<L.D	2	<L.D
Sr	155.5	133.2	191.5	162	166.5	169	196	303	115
Ta	0.1	0.1	<L.D	0.1	0.1	0.4	0.2	0.2	<L.D
Th	0.41	0.32	0.33	1.31	0.59	0.32	0.26	0.67	0.12
U	0.22	0.15	0.19	0.11	0.15	0.16	0.14	0.65	0.08
V	6	5	<L.D	<L.D	<L.D	5	<L.D	6	<L.D
W	33	28	<L.D	19	0.1	87	33	35	<L.D
Zr	4	2	2	9	14	3	3	23	<L.D

Table 3: Rare earth element and yttrium data (ppm) for all the marble study samples.

Locality	San Miguel marble, Tandilla System								
Sample #	SMC-1	SMC-2	SMC-3	SMC-4	SM-5	SMC-6	SMC-7	a-SMC	b-SMC
La	5.73	5.03	3.82	4.97	5.35	6.11	3.82	14.13	1.15
Ce	4.78	4.67	3.98	4.78	5.57	4.78	3.18	15.12	0.80
Pr	0.88	0.91	0.62	0.88	0.97	0.88	0.62	1.85	0.18
Nd	3.73	2.88	2.71	3.39	3.73	3.05	2.71	7.12	1.02
Sm	0.78	0.67	0.39	0.67	0.44	0.44	0.56	1.00	0.17
Eu	0.32	0.33	0.17	0.25	0.28	0.14	0.21	0.38	0.05
Gd	0.85	0.87	0.58	0.58	0.94	0.62	0.71	1.20	0.18
Tb	0.10	0.09	0.08	0.11	0.09	0.06	0.08	0.14	0.03
Dy	0.84	0.77	0.47	0.75	0.75	0.51	0.61	0.98	0.28
Y	10.26	10.33	6.21	9.72	9.72	7.02	8.10	10.26	3.24
Ho	0.18	0.16	0.11	0.17	0.18	0.10	0.16	0.22	0.05
Er	0.43	0.44	0.29	0.51	0.48	0.37	0.37	0.48	0.14
Tm	0.08	0.07	0.07	0.06	0.10	0.07	0.07	0.10	0.03
Yb	0.28	0.33	0.20	0.31	0.34	0.31	0.37	0.31	0.11
Lu	0.05	0.03	0.02	0.03	0.03	0.02	0.05	0.03	0.01
$\sum$REE	29.29	27.58	19.71	27.17	28.98	24.50	21.61	53.34	7.43
Y/Ho	57.52	64.56	56.97	57.70	54.49	70.84	51.08	47.06	65.39
LREE(Pr/Yb)$_{PAAS}$	1.00	0.88	1.00	0.91	0.92	0.91	0.54	1.91	0.50
MREE(Sm/Yb)$_{PAAS}$	1.40	1.03	1.00	1.09	0.67	0.73	0.77	1.64	0.75
Eu/Eu*$_{SN}$	2.40	2.97	2.13	2.09	2.74	1.53	2.11	1.79	1.67
Ce/Ce*$_{SN}$ Ce$_{SN}$/(0.5La$_{SN}$+0.5Pr$_{SN}$)	0.48	0.50	0.59	0.52	0.56	0.46	0.47	0.66	0.40
Ce/Ce*$_{SN}$ Ce$_{SN}$/(2Pr$_{SN}$+Nd$_{SN}$)	0.19	0.20	0.23	0.20	0.21	0.21	0.18	0.30	0.17

59

Pr/Pr*$_{SN}$ Pr$_{SN}$/(0.5Ce$_{SN}$+0.5Nd$_{SN}$)	1.18	1.44	1.08	1.25	1.22	1.33	1.17	1.05	1.33
La/La*$_{SN}$ La$_{SN}$/(3Pr$_{SN}$-2Nd$_{SN}$)	1.88	0.95	2.00	1.30	1.27	1.33	2.00	1.76	1.50

SN: Normalized to shale.

Table 4: Isotope composition of SM marble. $\delta^{13}C$ and $\delta^{18}O$ values from calcite relative to V-PDB (Vienna Pee Dee Belemnite) and to V-SMOW (Standard Mean Ocean Water), respectly. Also, $\delta^{18}O$ (V-SMOW) from diopside is presents.

Sample	$\delta^{18}O_{cal}$‰	$\delta^{13}C_{cal}$‰	$\delta^{18}O_{clpx}$‰	T °C
SMC-1	+17.45	+5.89	+14.50	623
SMC-2	+17.12	+5.42	+14.30	643
SMC-3	+16.80	+5.39	+14.10	663
SMC-4	+16.80	+5.06	n.d.	
SMC-5	+13.96	+5.05	n.d.	
SMC-6	+13.91	+4.95	n.d.	
SMC-7	+13.84	+4.26	n.d.	
a-SMC	+17.15	+5.42	n.d.	
b-SMC	+16.81	+4.94	n.d.	
c-SMC-	+17.05	+5.40	n.d.	

The SMC-7 to SMC-1 samples follow a core to rim marble cross-section, and a-SMC, b-SMC and c-SMC correspond to a rim-core-rim marble lenses sampling.

Table 5: Results of the Sm-Nd determinations in garnet-whole rock pairs from the San Miguel skarn.

Sample	Sm*	Nd*	$^{147}Sm/^{144}Nd$	$^{143}Nd/^{144}Nd$	$(^{143}Nd/^{144}Nd)_i$	$\varepsilon Nd_{(0)}$	T_{DM} (Ga)
Grt$_{SM-29}$	2.15	8.43	0.153973	0.511635	0.510501 ± 0.000009	-	-
WR$_{SM-29}$	2.03	9.03	0.136189	0.511504		-22.12	3.05
Grt$_{SM-31}$	0.81	5.72	0.085908	0.511031	0.481599 ± 0.000024	-	-
WR$_{SM-31}$	0.79	5.56	0.085707	0.510962		-32.69	2.47

*Sm and Nd contents are given in ppm

Highlights

- $\delta^{13}C$ >5‰ shows that San Miguel marble derived from a "Lomagundi-Jatuli" carbonate.

- $\delta^{13}C$ and $\delta^{18}O$ depletion was caused by Palaeoproterozoic metamorphic processes.

- Positive Y anomalies and HREE enrichment reflect marine precipitation conditions.

- Positive Eu anomalies manifest hydrothermal fluid participation in seawater.

- Ce negative anomaly indicates oxidizing precipitation conditions.